R. & M. No. 3187
(21,208)
A.R.C. Technical Report

R. & M. No. 3187

MINISTRY OF AVIATION

AERONAUTICAL RESEARCH COUNCIL
REPORTS AND MEMORANDA

Calculation of Flexible Wall Shapes and Preparation of Control Tapes for the Bedford 8-ft × 8-ft Wind Tunnel

By MARJORIE M. BARRITT
WITH AN APPENDIX BY K. V. DIPROSE

LONDON: HER MAJESTY'S STATIONERY OFFICE
1961
PRICE 13*s.* 0*d.* NET

Calculation of Flexible Wall Shapes and Preparation of Control Tapes for the Bedford 8-ft x 8-ft Wind Tunnel

By Marjorie M. Barritt

with an Appendix by K. V. Diprose

Communicated by The Deputy Controller Aircraft (Research and Development)
Ministry of Supply

*Reports and Memoranda No. 3187**
February, 1959

Summary.—This report describes an application of a digital computer to the aerodynamic design and automatic control of a large wind tunnel with flexible walls. The computational problem was threefold: first, calculation of the wall shapes for a set of 'pivotal' operating speeds between $M = 1$ and 2·8; second, computation of the necessary movements of the set of screw jacks which flex the walls; and finally, preparation of the set of digitally punched control tapes. A new mathematical approach was used for the first part in order to avoid singularities in the partial differential equations governing the flow in the convergent-divergent nozzle of the tunnel. The work was started in 1953 on the ACE Pilot Model at the National Physical Laboratory and completed on one of the Royal Aircraft Establishment DEUCE computers.

1. *Introduction.*—The air-speed in the working-section of a supersonic wind tunnel depends on the shape of the walls upstream of this section; in fact, the operating speed is determined solely by the ratio of the area of the working-section to that of the throat (Fig. 3). The usual practice in the past has been to fit a new wall section, or to insert linear blocks of appropriate shape, every time a change of tunnel speed was required. To avoid this cumbersome procedure a new method has been adopted for the 80,000 h.p. 8 ft × 8 ft Wind Tunnel at R.A.E., Bedford (Fig. 1) which is designed to operate at both subsonic and supersonic speeds (from $M = 0$ to $M = 2{\cdot}8$). The upper and lower walls of the adjustable part of this tunnel consist of flexible steel plates, each plate being 62 ft long, 8 ft wide and 1 in. thick (the two side walls are fixed at 8 ft apart). Each plate is supported and flexed by 30 pairs of screw jacks (shown diagrammatically in Fig. 2) driven by hydraulic motors and controlled by valves. The valves, in turn, are controlled electrically by means of punched paper tapes of standard teleprinter type, one tape for each jack. All the tapes move in unison under the control of electrical 'clock pulses' which occur at a rate of 390 pulses per minute, but the movement of any particular jack depends on the pattern of holes punched on the corresponding control tape[10].

This report discusses the computational problems arising in the automatic control of the flexible walls, first, calculation of the required wall shapes for a set of operating speeds between $M = 1$ and $M = 2{\cdot}8$ (these will be referred to as the 'pivotal design speeds'); then, computation of the necessary jack movements; and finally, preparation of the actual control tapes[12].

* R.A.E. Report M.S. 54, received 18th August, 1959.

The first stage entails the solution of the equations of flow in the convergent-divergent nozzle. The partial differential equations of flow are of the elliptic type where the flow is subsonic, that is, in the converging part of the nozzle upstream of the throat (Fig. 2), and hyperbolic in the diverging supersonic region. The usual tunnel design procedure is to use different mathematical techniques for dealing with the different flow regions. A linearised theory is used to relate the wall shape to the velocity distribution in the high subsonic and low supersonic region near the throat and the method of characteristics[1] is used to compute the shape of the supersonic part of the nozzle. The low-speed end of the subsonic part is very carefully designed to avoid unfavourable pressure gradients in the boundary layer and is then 'faired in' to the high subsonic region.

This method produces a very satisfactory single wall shape, but is not conducive to the production of a consistent family of wall shapes, particularly in the near-sonic part of the speed range. Some calculations on these lines were made in 1951, but failed to yield a sufficiently smooth and internally consistent set of 'pivotal' wall shapes. It was, however, shown by Diprose (Appendix I) that the differential equations of flow could be re-cast so that they had finite coefficients at all Mach numbers, with the boundary conditions specified in the same manner for all regions of the nozzle.

In this way the problem can be reduced to one of an 'initial value type', enabling a single numerical method, namely a step-by-step forward solution of the partial differential equations, to be used throughout. Furthermore, the co-ordinates of the wall shape (given by the wall streamline) can be produced in the course of the solution in a form suited to the final task, namely, the punching of the jack control tapes.

In the standard method for computing wall shapes the boundary conditions are usually given in terms of the velocity at exit (i.e., uniform flow at the required Mach number) and the desired radius of curvature of the wall at the throat. In the approach adopted by Diprose it is assumed that the wall shape is unknown, but that the flow is known in both direction and magnitude on one boundary, chosen in this case as the centre-line of the tunnel (the flow in the central vertical plane may be taken as two-dimensional and as symmetrical about the centre-line).

Starting on this basis the problem naturally breaks down into the following stages:

(1) Establishment of an arbitrary velocity distribution along the centre-line

(2) Calculation of the flow field for a set of operating speeds (the pivotal design speeds)

(3) Calculation of the corresponding wall shapes; that is, the evaluation of the cartesian co-ordinates of a set of points along the wall for each of the pivotal design speeds

(4) Calculation of the corresponding jack extensions and their sub-tabulation at small intervals of operating speed

(5) Preparation of the actual control tapes.

The work described in this report was spread over several years. Some stage (1) calculations, largely of an exploratory nature, were first done by hand, using desk calculating machines and graphical methods, but it soon became apparent that the aid of an automatic computer was desirable. At that time, about 1953, there was no such equipment at the R.A.E. and so the work was started on the ACE Pilot Model Computer at the National Physical Laboratory. The first set of control tapes was produced in this way in 1955. However, when the tunnel was set up, it was found necessary to make certain aerodynamic and engineering design alterations and most of the calculations were repeated. This part of the job was carried out between 1955 and 1957 on one of the R.A.E. DEUCE computers.

As both the ACE and DEUCE then used Hollerith cards for input and output, the final results had to be transcribed from cards to paper tape. In 1955 this was carried out at the R.A.E. on a 'mock-up' equipment and in 1957 at the University Mathematical Laboratory, Cambridge. One of the R.A.E. DEUCE computers is now equipped with tape output, thereby eliminating the need for this extra operation should any further work of this kind be undertaken.

2. *The Velocity Distribution along the Centre-line.*—It is necessary to represent the distribution of velocity along the centre-line by means of a mathematical formula, so chosen as to satisfy the physical and engineering conditions peculiar to this tunnel. In particular the height of the wall at entry (y_E in Fig. 3), the slope of the wall at entry, and the maximum allowable wall curvature at entry, are all prescribed by the general tunnel design. Three further considerations are: (i) the wall curvature at the throat must not exceed a specified maximum value, (ii) the exit velocity must be constant for a certain minimum distance ahead of the working section, and (iii) the wall shape must everywhere be a smooth curve.

If q is the magnitude of the flow velocity at any point and a is the velocity of sound at that point, then the Mach number M at that point is given by $M = q/a$. It is convenient to work in non-dimensional units, and so to define a specific speed (S) given by

$$S = \frac{q}{a_s}, \tag{1}$$

where a_s is the velocity of sound at the throat where the local Mach number is unity. The formula eventually chosen to represent the centre-line velocity distribution was

$$S = S_F - \left(\frac{S_F - S_E}{P}\right), \tag{2}$$

where

$$P = 1 + Ax + Bx^2 + Cx^4 + Dx^8 + Ef(x), \tag{3}$$

$$f(x) = \{\exp(\tfrac{5}{2}x) - \exp(-\tfrac{5}{2}x)\}^4. \tag{4}$$

The coefficients A, B, C, D and E are functions of the Mach number in the working-section, x denotes the length along the tunnel, and the suffixes $_E$, $_T$, and $_F$ refer to the conditions at entry, at the throat and at the working-section respectively (Fig. 3). The derivation of the coefficients in formula (3) is given in Appendix II; the basic assumptions on which these calculations were made are described here.

The approximate wall shape may be related to the centre-line velocity by assuming 'one-dimensional flow theory'[1]. It follows from the constancy of mass flow that the tunnel height is everywhere inversely proportional to the product of speed (S) and density (ρ). It is shown in Appendix I that

$$\frac{\rho}{\rho_0} = \left(1 - \frac{S^2}{6}\right)^{5/2}, \tag{5}$$

where ρ_0 is the density at the stagnation point, i.e., where $S = 0$. The values of S_F and S_E in (2) can then be expressed in terms of y_T, the half throat height, by the relationships

$$S_E\left(1 - \frac{S_E^2}{6}\right)^{5/2} y_E = S_T\left(1 - \frac{1}{6}\right)^{5/2} y_T = S_F\left(1 - \frac{S_F^2}{6}\right)^{5/2} y_F, \tag{6}$$

where $S_T = 1$ and the values of y_E and y_F are known.

The coefficient A is determined by the slope of the wall at entry, and B by the curvature of the wall at entry which was taken to be the maximum allowable. The curvature at entry is a maximum

at the lowest speed, i.e., $M = 1$. The curvature at the throat, on the other hand, is a maximum at the highest Mach number $M = 2{\cdot}8$. Fixing this value also by the curvature limits on the plates, together with assuming a position for the throat (estimated graphically), sufficed to determine the coefficients C and D.

The last two requirements mentioned in the first paragraph of this Section, namely, that 'the exit velocity must be constant for a minimum distance ahead of the working-section' and that 'the wall shape must be everywhere a smooth curve' are strictly speaking mutually inconsistent. An acceptable compromise was reached, however, by adding an exponential term $Ef(x)$ in equation (3) which allows an asymptotic approach to the final constant velocity in the working-section. The function $f(x)$ and coefficient E were chosen so that the effect of this additional term was negligible at entry but ensured that S converged to within 0·2 per cent of S_F at the point for which $x = 50$ ft (Fig. 3).

3. *Choice of 'Pivotal' Design Mach Numbers.*—To achieve the most economical use of the tape and to permit uniformity of sub-tabulation, it is desirable that the design speeds should be more or less equally spaced at equal steps of the fastest jack. It is reasonable to assume that this jack is near the throat and thus that this condition can be met by working initially in uniform steps of throat size, instead of equal intervals of Mach number. It will then be possible to revert to the latter for the master control tape by appropriate sub-tabulation of the original results.

Equations (6) express S_F and S_E in terms of y_T; the coefficients A, B, C, D, E can also be obtained in terms of this quantity. The approximate relationship between Mach number in the working-section, M_F, and y_T (Ref. 1, Vol. II, page 456) is

$$\frac{y_F}{y_T} = \frac{1}{M_F}\left\{\frac{5+M_F^2}{6}\right\}^3. \tag{7}$$

The total speed range ($M = 1$ to 2·8) was covered in two stages; in 4-in. steps of y_T from 13 in. to 45 in., and in 0·054-in. steps from 45 in. to 45·216 in. The very fine spacing near the speed of sound was chosen to enable accurate sub-tabulation to be carried out in this difficult region.

Table 1 shows the specific speeds and Mach numbers in the working-section corresponding to the final choice of 'pivotal' values of throat size.

TABLE 1

Half throat size (y_T) (in.)	Specific speed in working-section (S_F) (Equation (2))	Mach number in working-section (M_F) (Equation (7))
13	1·91227	2·793
17	1·82875	2·509
21	1·74869	2·280
25	1·66916	2·082
29	1·58759	1·903
33	1·50088	1·734
37	1·40391	1·564
41	1·28467	1·377
45	1·06315	1·077
45·054	1·05476	1·067
45·108	1·04469	1·054
45·162	1·03158	1·038
45·216	1·00000	1·000

4. *Evaluation of Velocity Flow Field.*—All the original calculations were made on the assumption of a constant rate of growth, independent of Mach number, of the displacement thickness of the boundary layer, of an amount 0·002 inch per inch, this being considered a sufficient estimate in the very early design stage. Later in the light of further experience a revised estimate was made by the method of Tucker[11]; this gave an average rate of growth which varied between 0·0015 and 0·0034 at different Mach numbers. The calculated ordinates of the pivotal wall shapes were then scaled to suit these corrections.

Once the centre-line velocity formula has been established the whole velocity field from the centre-line to the wall can be defined at some suitable mesh points for each of the design Mach numbers, i.e., the 'pivotal throat sizes'.

It is shown in Appendix I that the basic aerodynamic equations governing the flow can be expressed in the following form, where the notation is shown in Figs. 6 and 7:

$$\frac{\partial S}{\partial \psi} = \frac{S}{\left(1-\frac{S^2}{6}\right)^{5/2}} \frac{\partial \theta}{\partial \phi}, \tag{8}$$

$$\frac{\partial \theta}{\partial \psi} = \frac{-1(-S^2)}{S\left(1-\frac{S^2}{6}\right)^{7/2}} \frac{\partial S}{\partial \phi}. \tag{9}$$

From a computing point of view the stream function, ψ, is a satisfactory independent variable but the potential function, ϕ, is not, as its rate of change is so much greater in the supersonic than in the subsonic region. A change of variable was, therefore, desirable and the equations were rewritten as

$$\frac{\partial S}{\partial \psi} = \frac{S}{\left(1-\frac{S^2}{6}\right)^{5/2}} \frac{1}{S_A} \frac{\partial \theta}{\partial \xi}, \tag{10}$$

$$\frac{\partial \theta}{\partial \psi} = \frac{-(1-S^2)}{S\left(1-\frac{S^2}{6}\right)^{7/2}} \frac{1}{S_A} \frac{\partial S}{\partial \xi}, \tag{11}$$

where ξ is defined by the relationship

$$\frac{d\phi}{d\xi} = S_A, \tag{12}$$

the specific speed on the axis.

The calculations were then made on a ψ, ξ mesh, the velocity at the mesh points being expressed in terms of the specific speed S and the inclination θ of the velocity vector to the x axis (Fig. 6). Also on the centre-line of the tunnel $\xi = x$. The mesh intervals ($\delta\psi$ and $\delta\xi$) were so chosen that the wall streamline (less the boundary-layer correction) coincided with the ninth mesh streamline, counting out from the x axis. For computational purposes the mesh was extended to two streamlines beyond the wall, and to two equipotentials ξ beyond the point where the velocity became constant upstream of the working-section; this latter position, of course, varied for each Mach number.

Starting with the assumption that S and θ are known on one streamline (initially the centre-line), the derivatives normal to this streamline are computed from equations (10) and (11). By numerical integration S and θ are then found on the next streamline, and numerical differentiation along the streamline gives $\partial S/\partial \xi$ and $\partial \theta/\partial \xi$. Substitution of these new values in equations (10) and (11) enables the process to be repeated with a more accurate integration formula to give better values of S and θ

on this new streamline. In this manner, with the introduction of a special iteration cycle to improve estimated starting conditions, the whole velocity field is covered. Details of the formulae used are given in Appendix II. Selection of these formulae and choice of mesh size were only made after extensive preliminary investigations, carried out mainly on desk calculators. When a satisfactory plan had been evolved the calculations were programmed for the N.P.L. ACE Pilot Model and then subsequently re-programmed for the first R.A.E. DEUCE.

5. *Calculation of Wall Co-ordinates.*—An engineering limitation was that the stress in the flexible wall plates should not exceed 16 tons per square inch, with a further restriction on the bending moment of the sliding joint at the subsonic end of the plate (Fig. 3). If the curvature in the supersonic section is found to be unacceptably large, the only remedy lies in adjusting the centre-line formula. In the case of the subsonic region it is possible to carry out restricted smoothing mathematically so long as the process is applied identically to all pivotal values. This was, in fact, done as far as the first four jacks, to accommodate the requirements of the sliding joint and engineering alterations made after the computation of the wall ordinates. The rest of the nozzle proved satisfactory.

Knowing the values of S and θ at the ψ, ξ mesh points on the wall streamline, the cartesian co-ordinates x, y at these same points can be found by integration along the equipotentials from centre-line (ψ_0) to wall (ψ_ω). The relationships (Appendix I) are

$$x = \xi - \int_{\psi_0}^{\psi_\omega} \frac{\sin\theta}{S\left(1-\frac{S^2}{6}\right)^{5/2}} d\psi, \tag{13}$$

$$y = \int_{\psi_0}^{\psi_\omega} \frac{\cos\theta}{S\left(1-\frac{S^2}{6}\right)^{5/2}} d\psi. \tag{14}$$

Since it is now possible to check that the allowable wall curvature has not been exceeded, it is convenient in the same programme to compute $dl/d\xi$ and $d\theta/dl$, where l is defined as the distance from the fixed end of the plates in the working-section to some point on the wall (Fig. 8). The ratio $d\theta/dl$ gives the wall curvature, and integration of the quantity $dl/d\xi$ gives the distance l_i for each wall mesh point (x_i, y_i). We now have sufficient information to find the co-ordinates of the jack attachment points x_J, y_J, also shown in Fig. 8.

6. *Calculations of the Jack Extensions.*—Thirty pairs of screw jacks are attached to each wall of the tunnel, as shown in Fig. 2. The 'fixed' end of each jack is hinged about a fixed point whose co-ordinates (x_H, y_H) are specified on the contractor's drawings; the movable end is attached to a point on the wall by a pin joint whose co-ordinates (x_J, y_J) can now be determined (*see* Figs. 5 and 8). The extension of any jack (e) is given by the distance between these two points, which will be referred to as the hinge point and attachment point respectively. The method of computing the attachment point co-ordinates (x_J, y_J) and hence the extensions, is described in Appendix II.

At this stage the set of extensions (e) for each jack must be studied to establish whether the required relative movements of the various jacks will give optimum running conditions and further whether a sufficient number of pivotal wall shapes have been computed to permit a valid sub-tabulation scheme to be applied. In the case of the Bedford 8 ft Tunnel the first survey indicated that in fact these conditions were not likely to be fulfilled. Accordingly two lead screws were changed, namely, for jacks 19 and 20, and four additional wall shapes at intervals of 0·054 in. were computed in the Mach 1 region.

The tunnel system is designed so that each jack moves in steps of 0·0025 in. or 0·00125 in. as indicated in Fig. 4 and described in Ref. 10. As it had been decided that each possible jack movement was to be represented on the corresponding control tape, it was necessary to choose the sub-tabular intervals of throat size so that the distance between one value and the next did not result in any jack moving more than one step; in fact, this involved 17,408 steps of throat size for each of the 30 jacks. This extremely fine spacing means that, for practical purposes, the Mach number can be varied continuously over the speed range. For convenience in tunnel operation an additional critical table of Mach number against throat size was prepared. A master tape was then punched so that by a single switch the walls could be controlled and set in steps of 0·01 for Mach number. Full details of the sub-tabulation scheme are given in Appendix II.

7. *Conclusion.*—The tunnel calibrations so far carried out confirm that this new method of design has attained its objective of producing wall shapes that are both smooth in themselves and capable of smooth transition across the complete Mach-number range. Bearing in mind that the calculation was in every sense a pilot run (this was the first set of partial differential equations to be solved on ACE Pilot Model), the numerical work was accomplished without any major setbacks. This was undoubtedly due to the original decision to break down the problem into stages and to punch out or record results at each stage. The computed results of each stage were scrutinised by the aerodynamicist in charge of the tunnel design, and any obvious modifications incorporated immediately. This co-operation was invaluable; indeed, it can be said that the closest liaison between the aerodynamicists and the numerical analysts is an essential requisite of success in a project of this magnitude.

8. *Acknowledgements.*—The work described in this report was spread over a number of years and involved many people. The method of evaluating the flow field on a mesh of streamlines and equipotentials is due to K. V. Diprose. Much of the exploratory work on the form of a suitable centre-line distribution and choice of mesh size was carried out under his supervision by Mrs P. F. Wallis. The ACE Pilot Model programmes were prepared by N. A. Routledge; the DEUCE programmes by Mrs E. R. Woollett, D. G. Burnett-Hall and C. N. Linden; the EDSAC programme by Mrs E. N. Mutch of the Cambridge Mathematical Laboratory and the Pegasus programme by D. G. Burnett-Hall.

Continual co-operation was accorded by Bedford under the guidance of J. Y. G. Evans.

We should also like to express our thanks to the Director of the National Physical Laboratory and the staff of the Mathematics Division for the use of the ACE Pilot Model Computer, and to the Director and staff of the Cambridge University Mathematical Laboratory for the use of their card-to-tape transcription equipment and the EDSAC computer.

LIST OF REFERENCES

No.	*Author*	*Title, etc.*
1	L. Howarth (editor)	Modern Development in Fluid Dynamics: High Speed Flow. Vols. I and II. Oxford: Clarendon Press. 1953.
2	L. H. G. Sterne	Royal Aircraft Establishment, Bedford. *Nature*: Vol. 180. p. 775. October, 1957.
3	C. N. Linden	Deuce programs used in the calculation of wall shape for a supersonic nozzle. P. II. M.S. Computing Note B223.
4	H.M. Nautical Almanac Office ..	*Interpolation and Allied Tables.* H.M.S.O. 1956.
5	W. G. Bickley	Formulae for numerical integration. *Math. Gazette.* Vol. XXIII. p. 302. October, 1939.
6	F. B. Hildebrand	*Introduction to Numerical Analysis.* McGraw-Hill. 1956.
7	D. D. Wall	Note on predictor-corrector formulae. *Mathematical Tables and other Aids to Computation.* Vol. X. No. 55. July, 1956.
8	L. J. Comrie	*J. R. Statist. Soc.* Supplement 3. p. 87, 1936.
9	E. R. Woollett	Sub-tabulation with special reference to a high speed computer. *Quart. J. Mech. App. Math.* Vol. XI. Part 2. May, 1958.
10	T. Barnes and C. R. Durham ..	Automatic setting of the flexible walls of a large wind tunnel. *Proc. I.E.E.* Vol. 105. Pt. A. 1958.
11	M. Tucker	Approximate calculation of turbulent boundary-layer development in compressible flow. N.A.C.A. Tech. Note 2337. April, 1951.
12	S. H. Hollingdale and M. M. Barritt	An application of a computer to wind-tunnel design. *The Computer Journal.* Vol. 1. Pt. 1 and 2. 1958.
13	C. Robinson and S. J. M. Dennison	Interpretive and brick schemes with special reference to matrix operations. *Deuce Programme News.* No. 10. October, 1956.

APPENDIX I

Development of the Aerodynamic Equations of Flow

By K. V. Diprose, B.A.

1. *Notation* (*see also* Figs. 6 and 7).

l	Distance along a streamline
n	Distance along an equipotential
q	Magnitude of local velocity
θ	Direction of local velocity
ρ	Density
ρ_0	Stagnation value of ρ
p	Pressure
a	Speed of sound
a_0	Stagnation value of a
a_s	Value of a where the local Mach number is unity
γ	Ratio of specific heats (taken as 1·4)
S	Specific speed $\equiv q/a_s$
ϕ	Velocity potential $\equiv \int S\,dl$
ψ	Stream function $\equiv \int \rho/\rho_0\, S\,dn$
M	Mach number $= q/a$
x, y	Rectangular axes shown in diagram II; x is the axis of symmetry
ξ	A function of ϕ such that $d\phi/d\xi$ = specific speed (S_A) on the axis, $\psi = 0$. Then also $\xi = x$ on the axis

2. *The Equations of Fluid Flow.*—It is assumed that the flow is steady, irrotational, inviscid and adiabatic. Hence, in terms of distance along, and normal to, the streamlines, we have the following four equations:

Continuity:
$$\frac{\partial(\rho q)}{\partial l}+\rho q\frac{\partial \theta}{\partial n}=0. \tag{15}$$

Zero vorticity:
$$\frac{\partial q}{\partial n}-q\frac{\partial \theta}{\partial l}=0. \tag{16}$$

Conservation of momentum along the streamlines:
$$\frac{1}{\rho}\frac{\partial p}{\partial l}+q\frac{\partial q}{\partial l}=0. \tag{17}$$

Conservation of momentum across the streamlines:
$$\frac{1}{\rho}\frac{\partial p}{\partial n}+q^2\frac{\partial \theta}{\partial l}=0. \tag{18}$$

Integrating equation (17) gives $\int(dp/\rho+q^2/2)$ = a constant, say, K, independent of l, while integrating equation (18), after substituting for $\partial\theta/\partial l$ from equation (16) gives the similar result that K is independent of n. Hence K is constant everywhere.

We can establish these results in terms of the speed of sound, by considering equation (15) in one-dimensional flow, i.e., $\theta = 0$ everywhere.

Then

$$\rho\frac{\partial q}{\partial l}+q\frac{\partial \rho}{\partial l}=0.$$

Substituting for dq/dl from equation (17) gives

$$\frac{dp}{dl}-q^2\frac{d\rho}{dl}=0.$$

Hence $q^2 = dp/d\rho$ unless p and ρ are constant everywhere.

So $q=\sqrt{(dp/d\rho)}$ is the only speed at which a small jump in p and ρ can be maintained in steady flow.

This, then, must be the speed a of a plane wave.

The assumption of adiabatic flow implies that $p=\rho^\gamma C$ in a perfect gas, where C is a constant independent of the co-ordinates.

Hence

$$a^2=\frac{dp}{d\rho}=\gamma\rho^{\gamma-1}C$$

and

$$\int\frac{dp}{\rho}=\frac{\gamma}{\gamma-1}\rho^{\gamma-1}C=\frac{a^2}{\gamma-1},$$

so that

$$\frac{a^2}{\gamma-1}+\frac{q^2}{2}=K.$$

We are now in a position to express q and ρ in terms of a non-dimensional 'specific speed', S.

Let a_0 be the value of a when $q=0$, i.e., stagnation conditions, and a_s the value when $q=a$, i.e., on the sonic line.

Then

$$\frac{a^2}{\gamma-1}+\frac{q^2}{2}=K=\frac{{a_0}^2}{\gamma-1}=\frac{{a_s}^2}{\gamma-1}+\frac{{a_s}^2}{2}=\frac{1}{2}\frac{\gamma+1}{\gamma-1}{a_s}^2,$$

whence

$$\left(\frac{a}{a_0}\right)^2+\left(\frac{\gamma-1}{\gamma+1}\right)\left(\frac{q}{a_s}\right)^2=1.$$

If we define q/a_s as the 'specific speed', S, we get

$$\left(\frac{a}{a_0}\right)^2=1-\frac{\gamma-1}{\gamma+1}S^2.$$

If ρ_0 is the stagnation value of ρ then

$${a_0}^2=\gamma{\rho_0}^{\gamma-1}C,$$

so

$$\left(\frac{a}{a_0}\right)^2=\left(\frac{\rho}{\rho_0}\right)^{\gamma-1}$$

and

$$\frac{\rho}{\rho_0}=\left[1-\frac{\gamma-1}{\gamma+1}S^2\right]^{1/\gamma-1}.$$

Using the recommended value of 7/5 for γ, this reduces to

$$\frac{\rho}{\rho_0}=\left(1-\frac{S^2}{6}\right)^{5/2}\qquad\text{(Equation (5)).}$$

We can now go back and substitute in equations (15) and (16), in terms of S. It is convenient also at this point to introduce a potential function, ϕ, defined by

$$\frac{d\phi}{dl} = S, \tag{19}$$

and a stream-function ψ defined by

$$\frac{d\psi}{dn} = \frac{\rho}{\rho_0} S = S\left(1-\frac{S^2}{6}\right)^{5/2}. \tag{20}$$

Equation (15) then becomes

$$S\frac{\partial}{\partial\phi}\left[S\left(1-\frac{S^2}{6}\right)^{5/2}\right] + S^2\left(1-\frac{S^2}{6}\right)^{5}\frac{\partial\theta}{\partial\psi} = 0,$$

while equation (16) becomes

$$S\left(1-\frac{S^2}{6}\right)^{5/2}\frac{\partial S}{\partial\psi} - S^2\frac{\partial\theta}{\partial\phi} = 0.$$

These on reduction yield equations (8) and (9), namely,

$$\frac{\partial S}{\partial\psi} = \frac{S}{\left(1-\frac{S^2}{6}\right)^{5/2}}\frac{\partial\theta}{\partial\phi}$$

and

$$\frac{\partial\theta}{\partial\psi} = -\frac{(1-S^2)}{S\left(1-\frac{S^2}{6}\right)^{7/2}}\frac{\partial S}{\partial\phi}.$$

Given S and θ along one streamline, say, at $\psi = 0$, equations (8) and (9) allow the derivatives normal to this streamline to be calculated, and hence the value of S and θ to be found on another streamline by numerical integration. Differentiating these new values with respect to ϕ then allows the process to be repeated indefinitely.

For the purposes of numerical integration and differentiation, it is convenient to use equal increments of the independent variables. There is no difficulty with ψ, but the gradient $d\phi/dl$ is so much steeper in the supersonic region than in the subsonic, that it is very uneconomical in computing effort to take equal steps of ϕ. It is accordingly convenient to introduce a new variable ξ defined by equation (12), $d\phi/d\xi = S_A$, where S_A is the value of S at the point of intersection of the equipotential and the centre-line. Thus ξ is identical to l along this streamline, and equal increments of ξ are roughly equal increments of length along all streamlines.

In terms of ξ and ψ the equations of flow are given by equations (10) and (11), namely,

$$\frac{\partial S}{\partial\psi} = \frac{S}{\left(1-\frac{S^2}{6}\right)^{5/2}}\frac{1}{S_A}\frac{\partial\theta}{\partial\xi}$$

and

$$\frac{\partial\theta}{\partial\psi} = \frac{(1-S^2)}{S\left(1-\frac{S^2}{6}\right)^{7/2}}\frac{1}{S_A}\frac{\partial S}{\partial\xi}.$$

3. *Derivation of Wall Co-ordinates.*—From equation (20) we have

$$\frac{dn}{d\psi} = \frac{\rho_0}{\rho S}. \tag{21}$$

The inclination of the equipotential at any point to the y axis is equal to the inclination of the streamline to the x axis at that point. This is defined as θ, where positive θ corresponds to x decreasing with increasing n. Hence

$$\frac{dy}{dn} = \cos\theta$$

and

$$\frac{dx}{dn} = -\sin\theta,$$

yielding

$$\frac{dy}{d\psi} = \frac{\rho_0}{\rho S}\cos\theta$$

and

$$\frac{dx}{d\psi} = -\frac{\rho_0}{\rho S}\sin\theta.$$

Substituting for $\rho_0/\rho S$ in terms of S from equation (5) and integrating gives equations (13) and (14) of paragraph 5.

APPENDIX II

Numerical Methods

The contract specification stated that the required accuracy for the setting of the flexible walls was of the order of 0·005 in., so the numerical procedure was chosen with a view to attaining an accuracy of 0·001 in. in the wall shapes, i.e., within the discrete jack steps of 0·0025 in. and 0·00125 in.

Wherever possible automatic computing equipment was used to minimise errors and reduce the time taken for the project. The type of calculation involved was well suited to a high-speed computer.

1. *Centre-line Velocity Formula: Calculation of the Coefficients.*—The general principles on which the analytical formula for the centre-line was chosen are described in Section 2, but details of precise formulae used to determine the coefficients in equation (3) are given here. By substituting the actual tunnel dimensions into equations (6) we can solve for S_F and S_E for the design Mach numbers. It will be noted that although the nominal half-height of the working-section is 48 in., y_F is taken as 45·216 in. This is to allow for the initial boundary-layer assumptions mentioned in Section 4. Values of S_E and S_F given in Table 3 were thus computed from the equations

$$S_E\left(1-\frac{S_E^2}{6}\right)^{5/2}\times 86{\cdot}40 = S_T\left(1-\frac{1}{6}\right)^{5/2} y_T, \qquad (S_E<1),$$

$$S_F\left(1-\frac{S_F^2}{6}\right)^{5/2}\times 45{\cdot}216 = S_T\left(1-\frac{1}{6}\right)^{5/2} y_T, \qquad (S_F>1),$$

where $y_T = 13\ (4)\ 45$ in. and $45\ (0{\cdot}054)\ 45{\cdot}216$ in., and $S_T = 1$.

We can now determine the coefficients A, B, C, D, E.

The coefficient A depends on the shape of the wall at entry. Equation (2) is differentiated to give

$$\frac{dS}{dx} = \frac{(S_F-S_E)P'}{P^2}. \tag{22}$$

From equation (6) we have, at entry, throat and exit

$$\frac{dy}{dS} = -\frac{y(1-S^2)}{S\left(1-\frac{S^2}{6}\right)}. \tag{23}$$

Combining with (22) we then have

$$\left[\frac{dy}{dx}\right]_E = -\frac{y(1-S^2)}{S_E\left(1-\frac{S_E^2}{6}\right)}\frac{(S_F-S_E)P'}{P^2}, \tag{24}$$

$$\left[\frac{dy}{dx}\right]_{x=0} = -\frac{6y_E(1-S_E^2)(S_F-S_E)A}{S_E(6-S_E^2)}, \tag{25}$$

since at entry $x = 0$, so that $P = 1$ and $dP/dx = P' = A$.

The left-hand side of (25) is specified at $x = 0$ by the construction of the tunnel and A is found as

$$A = -\frac{S_E(6-S_E^2)}{6y_E(1-S_E^2)(S_F-S_E)}\left(\frac{dy}{dx}\right)_{x=0}. \tag{26}$$

The coefficient B depends on the curvature (τ) of the wall at entry. From (24), we have

$$\tau\left(1+\left(\frac{dy}{dx}\right)^2\right)^{3/2} = \frac{d^2y}{dx^2} \equiv -(S_F-S_E)\left[\frac{p(1-S^2)}{S\,1-\frac{S^2}{6}}\right]\times$$

$$\times\left\{\left[\frac{y'p'}{p^2}+\frac{yp''}{p^2}-\frac{2y(p')^2}{p^3}\right]-\left[\frac{6+3S^2+S^4}{6S^2\left(1-\frac{S^2}{6}\right)^2}y\frac{p'}{p^2}\frac{dS}{dx}\right]\right\}. \tag{27}$$

At entry this can be written as

$$\left(\frac{d^2y}{dx^2}\right)_{x=0} = -(S_F-S_E)y_E\left\{\frac{(1-S_E^2)}{S_E\left(1-\frac{S_E^2}{6}\right)}\left[-\frac{6(S_F-S_E)(1-S^2)}{S_E(6-S_E^2)}A^2+\right.\right.$$

$$\left.\left.+2B-2A^2-\frac{6+3S_E+S_E^4}{6S_E^2\left(1-\frac{S_E^2}{6}\right)^2}(S_F-S_E)A^2\right]\right\},$$

or

$$\tau_E\left(1+\left(\frac{dy}{dx}\right)^2\right)^{3/2} = (S_F-S_E)y_E\left[A^2\left\{\frac{(S_F-S_E)(12-9S_E^2+7S_E^4)}{6S_E^2\left(1-\frac{S_E^2}{6}\right)^2}+\frac{2(1-S_E^2)}{S_E\,1-\frac{S_E^2}{6}}\right\}-2B\right]. \tag{28}$$

The values A, S_E, S_F, y_E have already been obtained and τ_E and $(dy/dx)_{x=0}$ are specified by the tunnel design; B can thus be determined from (28).

The coefficients C and D are to be defined by the position of and curvature at the throat. Since the coefficient E is chosen so that the exponential term is negligible at the throat, where $S = 1$, equations (2), (3) give

$$\frac{S_F-S_E}{S_F-1} = P_T = 1+Ax_T+Bx_T^2+Cx_T^4+Dx_T^8, \tag{29}$$

where x_T denotes the position of the throat.

Now $(dy/dx)_{x=x_T} = 0$. Thus from (22) and (29) equation (27) can be written

$$\tau_T = (S_F-S_E)\frac{10y_T}{6(\frac{5}{6})^2}\left[\frac{p'}{p^2}\frac{dS}{dx}\right]_T = \frac{12}{5}\frac{(S_F-1)^4}{(S_F-S_E)^2}y_T(p')_T^2,$$

giving

$$P_T' = A+2Bx_T+4Cx_T^3+8Dx_T^7 = \sqrt{\left(\frac{5_T}{12y_T}\right)}\frac{(S_F-S_E)}{(S_F-1)^2}. \tag{30}$$

If the position x_T and curvature τ_T of the wall at the throat are specified, then (29) and (30) provide a pair of simultaneous equations from which C and D may be deduced.

The coefficient E is chosen to have negligible effect up to the throat but to ensure that S converges to within $\frac{1}{5}$ of 1 per cent of S_F upstream of the working-section, at the point $x = 50$ ft. Application of this criteria to the lowest and highest Mach-number cases, with substitution of $x = 2$ in equation (3) will give two limiting values of E. Interpolation between these will give the remaining values. Numerical values of the coefficients are given in Table 4.

2. *Estimation of Suitable Intervals for Equipotential and Streamline Mesh.*—From Appendix I and Section 4, we have S and θ defined at all points between the centre-line and wall streamline by

equations (10) and (11), namely,

$$\frac{\partial S}{\partial \psi} = \frac{S}{\left(1-\frac{S^2}{6}\right)^{5/2}} \frac{1}{S_A} \frac{\partial \theta}{\partial \xi},$$

$$\frac{\partial \theta}{\partial \psi} = -\frac{1-S^2}{S\left(1-\frac{S^2}{6}\right)^{7/2}} \frac{1}{S_A} \frac{\partial S}{\partial \xi}.$$

The main numerical problem lies in the solution of these equations (the choice of method is discussed in the next paragraph), which are to be solved numerically on a bivariate mesh of streamlines and equipotentials. The first task is to choose suitable intervals $\delta\psi$ and $\delta\xi$ (having in mind the method to be used for solution of the equations). The choice of intervals is critical; a poor choice may result in the build-up of round-off error swamping the true solution. In this problem, for the supersonic region, Diprose was able to establish a criterion for the ratio $\delta\psi$ to $\delta\xi$, by investigating the physical problem of the propagation of small disturbances in supersonic flow, using the method of characteristics. This yielded the same result as a numerical consideration of the propagation of errors in proceeding from row r to row $(r+1)$ of the mesh. The argument runs as follows:

Let $f_1(S)$ denote $\dfrac{S}{S\left(1-\frac{S^2}{6}\right)^{5/2}} \dfrac{1}{S_A}$, so that $\dfrac{\partial S}{\partial \psi} = f_1(S) \dfrac{\partial \theta}{\partial \xi}$,

and $f_2(S)$ denote $-\dfrac{1-S^2}{S\left(1-\frac{S^2}{6}\right)^{7/2}} \dfrac{1}{S_A}$ so that $\dfrac{\partial \theta}{\partial \psi} = f_2(S) \dfrac{\partial}{\partial \xi}$,

and let ξ_i be any equipotential on row r (streamline ψ_r),
ξ_i be the same equipotential on row $r+1$ (streamline ψ_{r+1}),
ϵ be a small error in S on row r.
On row (r) the maximum error in $\partial\theta/\partial\psi$ is

$$f_2(S_i)\frac{\epsilon}{\partial \xi} + \left(\frac{\partial S}{\partial \xi}\right)_i \epsilon \frac{\partial}{\partial S_i}[f_2(S_i)].$$

The second term is negligible compared with the first so that the error in

$$\frac{\partial \theta}{\partial \psi} \simeq \frac{\epsilon}{\partial \xi} f_2(S).$$

Therefore the error in

$$(\theta_{r+1} - \theta_r) = \delta\theta \simeq \frac{\partial \psi}{\partial \xi} \epsilon f_2(S)$$

and the error in

$$\frac{\partial S}{\partial \psi} \simeq f_1(S)\, \epsilon f_2(S) \frac{\delta\psi}{(\delta\xi)^2}.$$

The maximum increase in error is S, in going from row (r) to row $(r+1)$, is thus approximately

$$\epsilon f_2(S) f_1(S) \left(\frac{\delta\psi}{\delta\xi}\right)^2.$$

If we specify that this must not exceed the original error ϵ in S, we have

$$f_2(S)f_1(S)\left(\frac{\delta\psi}{\delta\xi}\right)^2 < 1,$$

i.e.,

$$\frac{\delta\psi}{\delta\xi} < \frac{S_A\left(1-\frac{S^2}{6}\right)^3}{(S^2-1)^{1/2}}. \tag{31}$$

The crucial quantity is $\delta\xi$ which affects the accuracy of the numerical differentiation used to obtain derivatives with respect to ξ in formulae (10) and (11). All numerical differentiation formulae start effectively with the first difference of the function, so that too small an interval means a noticeable loss of figures in the derivative. The use of a larger interval and higher-order formula is therefore recommended (the differences must, of course, converge). The precise number of figures required in the derivative, and hence the decision on the value of $\delta\xi$, depends on the number of figures (i.e., the precision) in the function S, which is governed by the contract specification of accuracy for the walls. In this case an accuracy of 0·005 in. was required, and so 0·0001 (in 300 inch units) was taken as the objective of the numerical work.

The precision required in S can be roughly estimated from the known dependence of y on S in one-dimensional flow (*see* equation (6)). This estimate had then to be generously increased to allow for build-up of round off errors in the subsequent computing and ultimately S and θ were taken to seven decimal places.

On the centre-line the analytic derivatives were obtained and used as a guide to determine $\delta\xi$. It was soon found that at a spacing of more than 25 in. no polynomial formula of any degree would give the derivatives to the required accuracy. After much experimental work on a desk machine $\delta\xi$ was fixed at 15 in. and the numerical differentiation formula truncated at the fourth difference.

With $\delta\xi$ fixed at 15 in., we can now consider $\delta\psi$. The right-hand side of (31) decreases steadily as S increases (if $S>1$), and so an upper bound to $\delta\psi$ can be set by consideration of conditions at the highest Mach number ($M = 2{\cdot}8$), where $S \simeq 1{\cdot}9$ (Table 1). This gives, using (31),

$$\frac{\delta\psi}{\delta\xi} < 0{\cdot}075,$$

so with $\delta\xi = 15$ in., $\delta\psi < 1{\cdot}125$ in.

The value of the wall streamline ψ_w can be derived from equation (20), which, for parallel flow, gives

$$\psi = S\left(1-\frac{S^2}{6}\right)^{5/2} y. \tag{32}$$

Application of this formula at the throat gives a relationship between ψ_w and y_T, where y_T is known and $S = 1$, i.e.,

$$\psi_w = y_T\left(1-\frac{1}{6}\right)^{5/2}. \tag{33}$$

To avoid interpolation for the wall streamline, $\delta\psi$ was varied for each pivotal value of y_T, and, in each case, made equal to $\frac{1}{9}\psi_w$, i.e., the ninth streamline of the mesh was identical with the wall streamline. Substitution in (33) for the highest Mach number gives

$$\delta\psi = \frac{1}{9}\left(1-\frac{1}{6}\right)^{5/2} \times 13 \simeq 0{\cdot}91,$$

which being less than 1·125 in. satisfies condition (31).

Similar checks were made for the other design Mach numbers with satisfactory results. The values of $\delta\psi$ are given in Table 5.

3. *Solution of the Partial Differential Equations of Flow.*—Appendix I shows how the equations of flow can be transformed into a pair of simultaneous first-order partial differential equations with 'initial value' conditions given. There was thus some choice in the method of solution, though little experience at that time (1953) of handling such processes on a high-speed computer. Some well-known methods, for example that of Runge-Kutta[6] which is much used on high-speed computers for solving ordinary differential equations, seemed to be unsuitable in this case. In fact, the most practicable class of methods appeared to be that of the 'predictor and corrector' iterative type (Ref. 4, page 72); backward difference, central difference or Lagrange type (ordinate) integration formulae may be used. For a desk machine the central difference form is preferable, but for a high-speed computer the process of estimation and correction of missing differences would lead to an unduly complicated programme without any great reward. In any case, for a high-speed computer the order of approximation must be specified in advance, and then checked by differencing the results; there is thus no immediate gain in using finite difference formulae, as the differences would only be formed inside the computer.

The actual formulae used were the same for both the ACE and DEUCE programmes; for the former they were evaluated in their finite difference form, and for the latter as Lagrange type. The change introduced considerable simplification into the DEUCE programme, as the application of each formula each time could be treated as a multiplication of vectors to give a scalar product. For this particular problem all formulae, including the differentiation formulae to obtain derivatives with respect to ξ at each mesh point, were truncated at the fourth difference term, i.e., were 'five-point' formulae, and thus the same sub-routine could be used to form all the scalar products. The truncation point was only selected as the result of considerable exploratory work on desk machines after the intervals $\delta\xi$ and $\delta\psi$ had been fixed in the manner described in Section 2. A separate DEUCE programme was prepared to evaluate differences up to the fourth so that the results could be checked in both the ξ and ψ directions at suitable check points in the range. Further, for each streamline, i.e., each row of the mesh, a 'compare card' was punched out giving the maximum difference between the predicted and corrected values of S or θ. The application of this will be described in Section 3.3.

In the ACE and early DEUCE programmes an attempt was made to impose boundary conditions in the ξ direction of the mesh, in addition to the initial conditions on the centre-line, in effect, to substitute cards with these boundary conditions in place of the end points of each row of the mesh produced by the iterative solution of the equations of flow. These boundary values were intended to produce solutions which would satisfy the entry and exit conditions of the tunnel. This attempt proved unsuccessful partly due to the fact that too drastic an approximation was used to compute the entry conditions and thus the boundary values did not represent the flow at entry, and partly due to the inherent difficulty of trying to satisfy an excessive number of boundary conditions. Undoubtedly the wall streamline of the mesh must satisfy the geometrical conditions of the tunnel, and if the step-by-step solution which depends directly on the original choice of centre-line distribution does not do this, then some final arbitrary smoothing may be necessary. This must obviously have negligible effect on the subsonic flow, and so the amount that can be tolerated will depend on the structure of the tunnel.

The later DEUCE programme catered solely for an initial-value problem, and the results were much more satisfactory. Some smoothing was still necessary to keep the curvature of the plates

below the entry conditions limits, which are more severe there than elsewhere due to the 'stepped' construction of the flexible plates. This smoothing was carried out by Aero Department, Bedford, and included the refined boundary-layer corrections which were applied to the computed jack extensions prior to sub-tabulation (of jack movements). The formulae used by this programme which are given below were applied in an iteration cycle to proceed from row to row of the mesh thus:

On any row r, S and θ are differentiated with respect to ξ by formula (34) ((35) and (36) for end points). These derivatives are then substituted in equations (10) and (11) to give $\partial\theta/\partial\psi$ and $\partial S/\partial\psi$ on row r; these values together with the value of S and θ on row r and the derivatives on the three previous rows $(r-1)$, $(r-2)$, $(r-3)$ are used in an extrapolation integration formula (37) to obtain predicted (approximate) values of S and θ on row $(r+1)$. Differentiation by formulae (34), (35), (36) provides $\partial S/\partial\psi$ and $\partial\theta/\partial\psi$ on row $(r+1)$, which in addition to the derivatives on rows r, $(r-1)$, $(r-2)$, $(r-3)$ and the function values S and θ on row r, are used in the 'corrector' integration formula (38) to give 'corrected' (more accurate) values of S and θ on row $(r+1)$.

There is no provision in the programme to repeat the iteration cycle. The reason for this is discussed in Section 3.3.

3.1. *Formulae Used in These Programmes* (*Notation as in Ref.* 4).

Differentiation with respect to ξ (f denotes S or θ; n is the number of points on the centre-line).

(a) *Interior points* ($\xi_2, \ldots, \xi_1, \ldots, \xi_{n-2}$)

$$\left.\begin{aligned} &ACE && f_0' = \frac{1}{\delta\xi}\left[\mu f_0 - \frac{1}{6}\mu\delta^3 f_0\right] \\ &DEUCE && f_0' = \frac{1}{12\delta\xi}\left[\mu f_{-2} - 8f_{-1} + 8f_1 - f_2\right] \end{aligned}\right\} \tag{34}$$

(b) *End points* (ξ_0, ξ_1 and ξ_{n-1}, ξ_n)

$$\left.\begin{aligned} &ACE && f_0' = \frac{1}{\delta\xi}\left[\Delta f_0 - \frac{1}{2}\Delta^2 f_0 + \frac{1}{3}\Delta^3 f_0 - \frac{1}{4}\Delta^4 f_0\right] \\ & && f_0' = \frac{1}{\delta\xi}\left[\Delta f_{-1} + \frac{1}{2}\Delta^2 f_{-1} - \frac{1}{6}\Delta^3 f_{-1} + \frac{1}{12}\Delta^4 f_{-1}\right] \\ & && f_0' = \frac{1}{\delta\xi}\left[\nabla f_0 + \frac{1}{2}\nabla^2 f_0 + \frac{1}{3}\nabla^3 f_0 + \frac{1}{4}\nabla^4 f_0\right] \\ & && f_0' = \frac{1}{\delta\xi}\left[\nabla f_{-1} - \frac{1}{2}\nabla^2 f_{-1} - \frac{1}{6}\nabla^3 f_{-1} - \frac{1}{12}\nabla^4 f_{-1}\right] \\ &DEUCE && f_0' = \frac{1}{12\delta\xi}\left[-3f_4 + 16f_3 - 36f_2 + 48f_1\right] - 25f_0 \\ & && f_0' = \frac{1}{12\delta\xi}\left[f_3 - 6f_2 + 18f_1 - 10f_0 - 3f_{-1}\right] \\ & && f_0' = \frac{1}{12\delta\xi}\left[-f_{-3} + 6f_{-2} - 18f_{-1} + 10f_0 + 3f_1\right] \\ & && f_0' = \frac{1}{12\delta\xi}\left[3f_{-4} - 16f_{-3} + 36f_{-2} - 48f_{-1} + 25f_0\right] \end{aligned}\right\} \tag{35}$$

Integration with respect to ψ (f denotes either $\partial\theta/\partial\psi$ or $\partial S/\partial\psi$; ψ_0 and ψ_1 refer to rows r_1 and $(r+1)$).

(a) The predictor formula (Adams-Bashforth[4]).

$$\left.\begin{aligned} &ACE && \int_{\psi_0}^{\psi_1} f\,d\psi = \left[f_0+\frac{1}{2}\nabla f_0+\frac{5}{12}\nabla^2 f_0+\frac{3}{8}\nabla^3 f_0+\frac{251}{720}\nabla^4 f_0\right] \\ &DEUCE && \int_{\psi_0}^{\psi_1} f\,d\psi = \frac{1}{720}[1901f_0-2774f_{-1}+2616f_{-2}-1274f_{-3}+251f_4] \end{aligned}\right\}. \tag{36}$$

(b) The corrector formula (Bickley[5]).

$$\left.\begin{aligned} &ACE && \int_{\psi_0}^{\psi_1} f\,d\psi = \frac{\delta\psi}{720}[251f_1+469f_0+109\nabla f_0+49\nabla^2 f_0+19\nabla^3 f_0] \\ &DEUCE && \int_{\psi_0}^{\psi_1} f\,d\psi = \frac{\delta\psi}{720}[251f_1+646f_0-264f_{-1}+106f_{-2}-19f_{-3}] \end{aligned}\right\}. \tag{37}$$

The results of these programmes were punched out a row at a time and the calculation was extended to two streamlines beyond the wall to permit integration along the equipotentials (*see* Section 4). The output consisted of two binary cards for each point and an optional decimal card with the configurations shown below.

Binary cards (in standard floating binary)

First card:

S_r on X and Y rows of the card

θ_r 0 and 1

S 2 and 3

$\frac{\partial S_{r-1}}{\partial\psi}$ 4 and 5

$\frac{\partial S_{r-2}}{\partial\psi}$ 6 and 7

$\frac{\partial S_{r-3}}{\partial\psi}$ 8 and 9.

Second card:

$\frac{\partial\theta_{r-1}}{\partial\psi}$ on X and Y rows of the card

$\frac{\partial\theta_{r-2}}{\partial\psi}$ 0 and 1

$\frac{\partial\theta_{r-3}}{\partial\psi}$ 2 and 3

P_{17} 4.

Decimal cards

One card $\begin{cases} S \text{ as a signed ten digit number, nine decimal places.} \\ \theta \text{ as a signed ten digit number, nine decimal places.} \end{cases}$

The existing programme reads back these binary cards to start the next iteration, but from a computer storage point of view this is unnecessary, so that as the attempt to introduce boundary-value conditions would not be repeated in any future application the programme would be modified to avoid this.

In order to start this process on the first row of the mesh, some assumptions regarding the derivatives $\partial S/\partial\psi$ and $\partial\theta/\partial\psi$ on the previous three rows must be made and then corrected by another iterative procedure carried out by a programme called 'pull-back'.

3.2. *Starting Procedure.*—The first row of the mesh is the centre-line, $\psi = 0$; to start the predictor-corrector process we assume that $\partial S/\partial\psi$ and $\partial\theta/\partial\psi$ are equal to the value on $\psi = 0$ for the preceding three rows $(r-1)$, $(r-2)$, $(r-3)$. Since $\theta = 0$ on $\psi = 0$ and we have computed S on $\psi = 0$ from the centre-line distribution formula, we have all the information necessary to use the main programme 168 to proceed to the second row of the mesh. Programme 172 converts a decimal centre-line and produces two binary cards making the necessary assumptions. In fact, we compute out to the fourth row and then, using the symmetry of the tunnel, reflect back these values by programme 190 (pull-back) to form revised rows $(r-1)$, $(r-2)$, $(r-3)$. Hence we establish an iterative cycle, using these revised rows we obtain more accurate results for rows $(r+1)$, $(r+2)$, and $(r+3)$. These are compared by programme 329, and the iterations repeated until agreement in S and θ is reached to the required accuracy.

3.3. *Accuracy of the Results.*—As mentioned in Section 3.1 the main programme 168 punches out a 'compare card' which can be used as an estimate of the maximum error in S or θ, on that row of the mesh. The error terms in the predictor and corrector formulae are respectively

$$(\delta\psi)^6\frac{95}{288}f^{(v)}(Z) \quad \text{and} \quad (\delta\psi)^6\frac{3}{160}f^{(v)}(Z),$$

where (Z) is some point in the range of integration. The error of the 'predictor' is thus about 17 times as large as that of the 'corrector'. If, therefore, ϵ is the maximum acceptable error in the final values of S or θ (e.g., five units in the seventh decimal place) then the value of the compare card must not exceed 16ϵ. For this reasoning to be valid the functions must be 'well behaved' mathematically. It is essential that differencing checks should be carried out on the final results. In fact, on the compare card the values were always well below the prescribed maximum, and the corrector formula proved stable in application to these equations.

If the value on the compare card had been too high, then the intervals $\delta\xi$ and $\delta\psi$ would have had to be reduced. If the differences are too large then either higher-order formulae could be used, or again the intervals reduced. A change in the iteration cycle could be tried and a second application of the corrector formula made to see if the value on the compare card would be reduced. Wall[7] has shown that this is not always effective.

The predictor formula only provides the first approximation; the accuracy of the answer is entirely dependent on the 'corrector' formula. In these programmes the formulae (36) were actually truncated at the second difference term. This did not, in fact, save any appreciable computation time and it would have been simpler in the DEUCE programme to have used a five-point formula and thus avoided an additional sub-routine. There is no reason to suppose that this would not have been satisfactory, although there are occasions when inclusion of higher-order difference worsens the situation[7]. It should be recognised that, in the early days, time for experiment on ACE was severely limited (and so was the department's desk computing capacity). Moreover, the unexpected re-programming for DEUCE was carried out under extreme pressure to finish the calculations in advance of the completion of the structure so that delay in arrival of the new control tapes would not hold up calibration and use of the tunnel. Looking back on the job, it is now possible to suggest several other simple modifications to these programmes which would yield additional saving of computation time.

4. *Calculation of Wall Co-ordinates in X, Y Plane.*—We now have the values of S and θ at all points on the (ξ, ψ) mesh (and by symmetry in the corresponding region $\psi < 0$) which will enable any mesh point to be expressed in cartesian co-ordinates and, in particular to achieve the first objective, the calculation of the co-ordinates of the thirteen pivotal wall shapes.

Integration along the equipotential lines from the centre-line to the wall gives the required co-ordinates (x_i, y_i), of the point of intersection of each equipotential (ξ_i), with the wall streamline ψ_w, using equations (13) and (14).

Programme 377 carries out this integration numerically using formula (38), the truncation point again being decided after trial calculations on a desk machine (for Notation, *see* Ref. 4).

If we denote

$$f = \frac{\partial x}{\partial \psi} \quad \text{or} \quad \frac{\partial y}{\partial \psi}; \qquad \psi_n = \psi_w = \psi_9,$$

then
$$\int_{\psi_0}^{\psi_n} f \, d\psi = \left[\frac{1}{2} f_0 + f_1 + f_2 \ldots + f_{n-1} + \frac{1}{2} f_n + \frac{1}{12}(\mu \, \delta f_0 - \mu \, \delta f_n) - \frac{11}{720}(\mu \, \delta^3 f_0 + \mu \, \delta^3 f_n)\right]. \qquad (38)$$

This programme also computes $dl/d\xi$ and $d\theta/dl$ for each point $x_i y_i$ for use in the next stage of the calculations, where l is now the distance along the wall measured from the fixed downstream end of the plates, $x = 62$ ft, as shown in Fig. 9. The input for programme 377 consists of a set of the first card of the pair of binary cards from 168, re-ordered by columns instead of by rows (on a Hollerith sorting machine). The output is three cards for each point on the wall; the first has x, y, $dl/d\xi$ and $d\theta/dl$ in binary, and the other two have the same quantities in decimal.

4.1. *Curvature Check.*—The wall curvature was then computed as the ratio of $d\theta/d\xi$ to $dl/d\xi$ from the output of 377 and checked against the prescribed limits.

5. *Calculation of Jack Extensions.*—We are now in a position to determine the co-ordinates (x_J, y_J), Table 7, of the moving end of the jacks for each wall shape. As mentioned in Section 6, the contractor's drawings give (x_H, y_H), the co-ordinates of the fixed hinge points. The distance between these two points is the required jack extension (e).

The distance l_J along the wall streamline from the fixed downstream end of the plates to each attachment point (x_J, y_J) is specified on the contractor's drawings (Table 6). The distance l_i to each point (x_i, y_i) in the wall streamline can be computed by integration of $dl/d\xi$ punched out by the last programme (*see* Fig. 8). Thus for each design Mach number we now have a table of (x_i, y_i) against an argument l_i. Suitable interpolation into this table for each l_J will, therefore, give (x_J, y_J) for each of the thirteen pivotal wall shapes. As the argument l_i is at unequal intervals, an iterative interpolation method due to Aitken[4] suited both the problem and the computer, programme 409.

From the thirteen sets of thirty values of (x_J, y_J) and the known (x_H, y_H) (Table 6) we can compute the extensions, e. The actual values of (x_J, y_J) were scaled to accommodate various tunnel design modifications before the extensions (e) were computed on desk machines. The values of e for each jack were differenced to check that the relative rates of movement would be economical and that a reasonable sub-tabulation scheme for these values could be evolved. Originally only nine pivotal wall shapes were prepared, but a study of the first set of data soon revealed that this was inadequate, and further that the existing choice of lead screws would make the tunnel operation very slow. Accordingly, additional wall shapes were computed near the speed of sound, and two lead screws were changed. In fact, the general sub-tabulation scheme would have been simpler, and more firmly based, if the interval of y_T had been reduced throughout the range and extended

beyond the required maximum Mach number. It is probable that the total time taken would not have been longer once the DEUCE programmes had been linked together and unnecessary reading in of cards eliminated.

6. *Calculation of Jack Movements.*—The jacking system[10] is designed so that each jack moves in discrete steps of either 0·0025 in. or 0·00125 in. dependent on its position (*see* Fig. 4). The jack extensions required to set the tunnel to the pivotal wall shapes are, as we have seen, tabulated against an argument y_T. If these extensions are now expressed in units of jack movement and sub-tabulated to a very fine interval of y_T, it will be possible to ensure that no jack is required to move more than one step for any one change of wall setting, and for practical purposes the Mach number change will be continuous from 1 to 2·8. Jack movements were in fact computed for 17,408 steps of throat size y_T for each jack.

TABLE 2

Half throat size	Sub-tabular interval ratio	
	Stage I	Stage II
13	$\frac{1}{10}$	2^{-8}
17	$\frac{1}{9}$	2^{-8}
21	$\frac{1}{15}$	2^{-7}
25	$\frac{1}{15}$	2^{-7}
29	$\frac{1}{8}$	2^{-8}
33	$\frac{1}{8}$	2^{-8}
37	$\frac{1}{8}$	2^{-8}
41	$\frac{1}{8}$	2^{-8}
45	$\frac{1}{8}$	2^{-8}
45·054	—	2^{-6}
45·108	—	2^{-6}
45·162	—	2^{-6}
45·216	—	2^{-6}

The sub-tabulation scheme was kept as flexible as possible to enable changes in requirements to be incorporated in the light of experience without requiring a new DEUCE programme to be prepared. For this reason the work was carried out in two stages. For the second a special programme based on Comrie's method of 'bridging differences'[8] which uses Everett's interpolation formula[4], was prepared in advance, and for the first the Lagrangian interpolation formulae using standard matrix manipulation programmes with the ACE and DEUCE general interpretive scheme[13] were used.

In the bridging difference programme Everett's interpolation formula was truncated at the fourth difference, which was 'thrown back' on to the second. The main advantages of this method are that there is no loss of accuracy due to build-up of round-off error, and most of the multiplications normally associated with interpolation are replaced by additions, a considerable time-saving factor. Essential to Comrie's interpretation of the method is that for binary arithmetic (ACE and DEUCE are binary machines) α must be of the form 2^{-a} (where a is any integer, h is the original interval of tabulation, αh is the sub-tabular interval). For decimal arithmetic α is of the form $2^{-a}5^{-b}$ (b is also an integer). Based on considerations of the possible movement of the throat from one pivotal shape to the next, α was chosen initially as 2^{-8}, and the programme was arranged so that a simple alteration would cover a change to 2^{-5}, 2^{-6} or 2^{-7}. Programmes were prepared for both ACE and DEUCE.

The time taken to change Mach-number settings in the tunnel is solely dependent on the time taken by the reading equipment to read the corresponding length of tape. Operating times should obviously be kept down (to about 45 minutes for changing from Mach 1 to 2·8), and so the stationary portions on the tapes should be kept to a minimum. The pattern of holes on the tape will be governed by the choice of sub-tabular ratios. On the other hand, it is no use producing tapes without any blank spaces, as obviously sundry small adjustments will be required in the course of time and it is desirable that these can be made on the spot without retabulating and repunching the whole installation of tapes.

An effort was made to meet these conflicting requirements by a varied choice of sub-tabular intervals in Stage I, based on trial-and-error tactics, in conference with the tunnel aerodynamicists. The outcome is shown in Table 2.

Six-point Lagrangian interpolation formulae were used for Stage I (coefficients to nine decimal places, or exact wherever possible). The Lagrangian coefficients were treated as a matrix, and each of the thirty sets of nine pivotal values as a vector. The problem was then formulated for use of standard matrix multiplication 'bricks' of ACE and DEUCE Scheme A[13].

7. *Preparation of the Control Tapes.*—The programme for Stage II was constructed, so that the output was in a suitable form for direct transcription on to five-channel punched paper tapes. Separate sections of the programme checked this output before the transcription, and further checking programmes were prepared to check the tapes on either the Cambridge University EDSAC, or R.A.E. Pegasus, machines which have tape input and output (whereas DEUCE normally has card input and output). One of the R.A.E. DEUCE's has now been modified so that tape output can be fitted, thus in any future work of this kind the transcription stage would be avoided (there are occasions when card output is pre-eminently suitable, others when tape is preferable and many applications where the choice is immaterial).

The first set of tapes was transcribed in the R.A.E. The second set, which embodied the improved boundary-layer corrections, was prepared at the University Mathematical Laboratory, Cambridge as the R.A.E. equipment had been dismantled for another project. In each case the transcription was carried out at least twice to locate random errors; the second set was also checked on the EDSAC or Pegasus to detect systematic errors in view of the experience gained in production of the original tapes. The demand of the tunnel designers for a continuous length of 'error free' tape of over 17,000 characters was very hard to meet with the standard tape punching equipment then available.

The code selected to represent jack movements on the tapes was simple, but involved long stretches of blank tape for the more slowly moving jacks. This, too, is apparently not conducive to reliability of the tape reading equipment. The code used was:

Channel 1—lower wall—moving out (away from the centre-line of the tunnel)

Channel 2—lower wall—in

Channel 3—used for supersonic diffuser stations (on the first eight jacks only)

Channel 4—upper wall—in

Channel 5—upper wall—out.

The system is described in Ref. 10 and Fig. 9 shows a Hollerith card and the corresponding section of tape.

The jack movements were punched on the Hollerith cards in the form of thirty-two first differences of jack extensions (in units of jack movement). The Y row represented movements of the wall in

i.e., channels 2 and 4; the X row movements out, channels 1 and 5. The latter were almost non-existent, only on a very rare occasion was it necessary to retract any jacks whilst others were extending. The datum was the Mach 1 position of the plates. To lower the Mach number the tapes pass through the readers in the reverse direction and the functions of channels 1 and 2, and 4 and 5, are interchanged by reversing a relay[10].

Thus, with the exception of pivotal values required for checking purposes, the DEUCE output was restricted to first differences of jack extensions expressed in discrete steps of jack movement. The sub-tabular intervals of Stages I and II were chosen so that these first differences would be $+1$, 0 or -1, and tables were prepared against an argument of throat size, y_T. The final set of thirty tapes would suffice to operate the tunnel smoothly over the complete speed range in regular intervals of y_T, whereas it is more convenient to have an operational scale in equal intervals of Mach number. Therefore, a critical table of Mach number against y_T at intervals of 0·01 in Mach number was prepared; from this a master tape was punched and linked with the jack tapes so that all jacks can be set simultaneously to a specified Mach number.

8. *Conclusion: Computer Time Required.*—To compute one pivotal wall shape, using the programmes as they now exist, requires about $2\frac{1}{2}$ hours on DEUCE. If, however, the modifications recommended in the report sections were made, and the individual programmes linked together then with a mesh of 50×12 points, the time would be reduced to two hours. The sub-tabulation for one jack, including the punching out of every thirty-second function value for checking and information purposes, occupies about 30 minutes; this would go down to about 15 minutes if the intervals of y_T were reduced in accordance with suggestions in Section 6. The information for one jack occupies 544 Hollerith cards (32 values on one card) which can be transferred as 17,408 characters onto creed punched paper tape in one hour. This transcription time would in future be eliminated by the use of tape output on DEUCE. To read and check such a tape by EDSAC or Pegasus occupied 20 minutes.

To sum up, the programmes prepared for this job will accept data to nine decimal digits. All finite difference formulae are truncated at the fourth difference, thus the intervals of $\delta\psi$ and $\delta\xi$ must be such that fifth differences are negligible and at the same time satisfy the inequality (31). In the case of sub-tabulation by the method of bridging differences the fifth differences are also neglected, so that either sufficient pivotal wall shapes must be computed so that δy_T is small enough for this condition to be satisfied, or a preliminary sub-tabulation using a higher-order formula must be carried out.

TABLE 3

Specific Speed at Entry and Exit of the 8-ft × 8-ft Wind Tunnel

Half throat height (y_T) (in.)	13	17	21	25	29	33	37	41	45	45·054	45·108	45·162	45·216
At entry (S_E)	0·10252	0·13448	0·16680	0·19958	0·23292	0·26694	0·30183	0·33773	0·37487	0·375387	0·375899	0·376410	0·37619
At exit (S_F)	1·91227	1·82875	1·74869	1·66916	1·58759	1·50089	1·40391	1·28467	1·06315	1·054764	1·044693	1·031585	1·00000

These values were based on the following dimensions taken from the contractor's drawings:

(a) The effective half height of the working-section after subtraction of the displacement thickness of the boundary layer is taken to be 45·216 in.

(b) The half height of the tunnel at the origin, Fig. 2, is taken as 86·400 in.; converging at an angle of $\tan^{-1} 0{\cdot}47118$.

TABLE 4

Coefficients for Centre-line Formula (For use with x Measured in Units of 300 in.)

Half throat height (y_T) (in.)	13	17	21	25	29	33	37	41	45	45·054	45·108	45·162	45·216
A	0·092664	0·129852	0·172506	0·222192	0·281304	0·353928	0·448068	0·583494	0·891078	0·903993	0·919549	0·939942	0·989692
B	0·159930	0·217738	0·279677	0·346621	0·419900	0·502546	0·602851	0·747993	1·205134	1·231102	1·263351	1·307218	1·422410
C	0·497385	0·546674	0·597135	0·650962	0·710805	0·780835	0·869527	1·000806	1·419655	1·422232	1·424965	1·428446	2·660917
D	0·390426	0·489006	0·589927	0·697580	0·817266	0·957327	1·134711	1·397268	2·234966	2·240289	2·245586	2·252549	4·717491
10^6E	0·81	1·11020	1·53310	2·16316	3·17189	4·96418	8·75416	20·2712	295·358	300·4279	305·5609	312·4407	330·0000

TABLE 5

Values of Wall Streamline ψ_w

Half throat height (y_T) (in.)	13	17	21	25	29	33	37	41	45	45·054	45·108	45·162	45·216
ψ_w	0·0274707	0·0359232	0·0443751	0·0528282	0·0612808	0·0697332	0·0781857	0·0866383	0·0950908	0·0952048	0·0953189	0·0954330	0·0955472
$\delta\psi = \frac{1}{9}\psi_w$	0·00305230	0·00399147	0·00493057	0·00586980	0·00680898	0·00774813	0·00868730	0·00962648	0·01056564	0·01057831	0·01059099	0·01060367	0·01061636

TABLE 6

Contractor's Specification for Jack Attachment and Hinge Points (See Fig. 8)

Jack number	l_J (in.)	Jack number	x_H (in.)	y_H (in.)
2	744	2	52	127
3	714	3	79	127
4	684	4	110	127
5	654	5	135	127
6	624	6	161	$120\frac{1}{2}$
7	594	7	186	$102\frac{3}{8}$
8	564	8	212	100
9	540	9	234	100
10	516	10	256	100
11	492	11	278	100
12	468	12	300	100
13	444	13	323	100
14	423	14	$343\frac{1}{4}$	100
15	402	15	$363\frac{1}{2}$	100
16	381	16	$383\frac{3}{4}$	100
17	360	17	404	100
18	339	18	425	100
19	318	19	446	100
20	297	20	467	100
21	276	21	488	100
22	255	22	509	100
23	234	23	530	100
24	213	24	553	100
25	192	25	576	100
26	168	26	600	100
27	144	27	624	100
28	120	28	648	100
29	96	29	672	100
30	72	30	696	100
31	48	31	720	100

TABLE 7

Co-ordinates of Jack Attachment Points (Revised Boundary-Layer Corrections Included)

y_T'' / $x_J'' y_J''$	13″		17″		21″		25″		29″	
Jack number	x	y	x	y	x	y	x	y	x	y
2	13·476	80·439	12·047	81·147	10·728	81·812	9·550	82·412	8·343	82·975
3	40·282	66·970	39·079	68·137	37·918	69·133	36·825	70·028	35·806	70·900
4	67·371	54·079	66·418	55·784	65·514	57·367	64·651	58·818	63·846	60·236
5	95·246	42·989	94·509	45·255	93·797	47·362	93·110	49·326	92·474	51·266
6	123·845	33·929	123·249	36·653	122·665	39·202	122·109	41·641	121·603	44·091
7	152·986	26·798	152·472	29·866	151·972	32·789	151·508	35·666	151·096	38·596
8	182·526	21·567	182·052	24·865	181·596	28·052	181·183	31·259	180·823	34·559
9	206·329	18·498	205·871	21·924	205·437	25·294	105·049	28·727	204·714	32·279
10	230·202	16·036	229·759	19·610	229·345	23·199	228·978	26·879	228·661	30·679
11	254·130	14·177	253·701	17·944	153·304	21·798	252·952	25·764	252·646	29·833
12	278·112	13·251	277·692	17·287	277·301	21·449	276·952	25·698	276·645	29·981
13	302·112	13·307	301·688	17·741	301·287	22·260	300·928	26·763	300·616	31·148
14	323·092	14·211	322·644	19·098	322·221	23·923	321·853	28·536	321·548	32·841
15	344·018	15·971	343·526	21·322	343·084	26·321	342·725	30·850	342·448	34·892
16	364·856	18·575	364·324	24·228	363·893	29·149	363·571	33·392	363·338	37·035
17	385·600	21·838	385·071	27·476	384·686	32·087	384·420	35·905	384·238	39·079
18	406·290	25·433	405·815	30·743	405·497	34·899	405·292	38·218	405·158	40·907
19	426·982	29·017	426·589	33·814	426·343	37·437	426·193	40·257	426·099	42·474
20	447·713	32·367	447·407	36·576	447·225	39·657	447·122	41·984	447·060	43·760
21	468·497	35·370	468·270	38·967	468·142	41·527	468·074	43·403	468·035	44·792
22	489·334	37·983	489·173	40·987	489·086	43·057	489·044	44·533	489·020	45·593
23	510·216	40·205	510·107	42·650	510·050	44·291	510·025	45·418	510·011	46·203
24	531·135	42·048	531·064	43·991	531·028	45·256	531·014	46·094	531·006	46·659
25	552·081	43·544	552·037	45·052	552·015	45·996	552·008	46·601	552·003	46·998
26	576·044	44·885	576·019	45·974	576·007	46·625	576·004	47·024	576·001	47·278
27	600·023	45·898	600·010	46·649	600·003	47·073	600·002	47·327	600·000	47·484
28	624·011	46·646	624·005	47·137	624·001	47·399	624·001	47·549	624·000	47·645
29	648·005	47·192	648·002	47·488	648·000	47·637	648·000	47·718	648·000	47·775
30	672·002	47·588	672·001	47·745	672·000	47·819	672·000	47·858	672·000	47·890
31	696·000	47·883	696·000	47·942	696·000	47·967	696·000	47·981	696·000	47·995

y_T'' / $x_J'' y_J''$	33″		37″		41″		45″		45·216″	
Jack number	x	y	x	y	x	y	x	y	x	y
2	7·259	83·519	6·247	84·042	5·308	84·550	4·431	85·063	4·374	85·095
3	34·875	71·799	34·027	72·718	33·528	73·650	32·543	74·588	32·483	74·614
4	63·108	61·657	62·447	63·109	61·873	64·640	61·369	66·276	61·322	66·349
5	91·903	53·237	91·418	55·320	91·014	47·515	90·702	59·985	90·864	60·195
6	121·162	46·611	120·798	49·251	120·522	52·104	120·343	55·361	120·338	55·654
7	150·744	41·620	150·462	44·775	150·262	48·162	150·155	52·002	150·152	52·320
8	180·524	37·999	180·293	41·593	180·134	45·398	180·060	49·619	180·058	49·938
9	204·438	35·964	204·227	39·811	204·086	43·878	204·024	48·299	204·022	48·629
10	228·399	34·606	228·199	38·663	228·066	42·880	228·007	47·413	228·006	47·748
11	252·391	33·972	252·194	38·166	252·061	42·404	252·001	46·871	252·001	47·266
12	276·389	34·230	276·192	38·399	276·061	42·477	276·000	46·663	276·000	47·029
13	300·364	35·3[illegible]	300·176	39·281	300·055	42·999	300·000	46·678	300·000	46·956
14	321·313	36·79[illegible]	321·147	40·391	321·044	43·669	321·000	46·774	321·000	46·961
15	342·246	38·465	342·111	41·620	342·031	44·400	342·000	46·882	342·000	46·998
16	363·178	40·152	363·077	42·820	363·020	45·090	363·000	46·987	363·000	47·054
17	384·120	41·713	384·049	43·900	383·011	45·688	384·000	47·079	384·000	47·117
18	405·076	43·071	405·029	44·812	405·005	46·178	405·000	47·165	405·00;	47·184
19	426·046	44·201	426·016	45·548	426·002	46·556	426·000	47·241	426·000	47·251
20	447·008	46·119	447·000	46·846	447·000	47·846	447·000	47·313	447·000	47·319
21	468·014	45·808	468·003	46·549	468·000	47·058	468·000	47·384	468·000	47·387
22	489·007	46·340	489·001	46·869	489·000	47·220	489·000	47·452	489·000	47·454
23	510·003	46·736	510·000	47·106	510·000	47·347	510·000	47·521	510·000	47·521
24	531·001	47·031	531·000	47·285	531·000	47·452	531·000	47·587	531·000	47·587
25	552·000	47·250	552·000	47·425	552·000	47·540	552·000	47·652	552·000	47·652
26	576·000	47·438	576·000	47·552	576·000	47·639	576·000	47·725	576·000	47·725
27	600·000	47·583	600·000	47·661	600·000	47·722	600·000	47·797	600·000	47·797
28	624·000	47·705	624·000	47·758	624·000	47·805	624·000	47·867	624·000	47·867
29	648·000	47·813	648·000	47·850	648·000	47·886	648·000	47·936	648·000	47·936
30	672·000	47·913	672·000	47·939	672·000	47·964	672·000	48·003	672·000	48·003
31	696·000	48·009	696·000	48·025	696·000	48·041	696·000	48·068	696·000	48·068

TABLE 8

Centre-line Velocity Distributions (S_A)

y_T'' / ξ 300″ units	13″	17″	21″	25″	29″	33″	37″	41″	45″	45·054″	45·108″	45·162″	45·216″
0·00	0·10252	0·13448	0·16680	0·19958	0·23292	0·26694	0·30183	0·33773	0·3748756	0·3753868	0·3758986	0·3764102	0·3769191
0·05	0·11159	0·14633	0·18142	0·21698	0·25310	0·28991	0·32759	0·36628	0·4061395	0·4066808	0·4072275	0·4077724	0·4083128
0·10	0·12206	0·15988	0·19799	0·23648	0·27545	0·31498	0·35526	0·39635	0·4382062	0·4387567	0·4393128	0·4398608	0·4404192
0·15	0·13409	0·17525	0·21656	0·25809	0·29991	0·34205	0·38450	0·42767	0·4706423	0·4711687	0·4716958	0·4721974	0·4728209
0·20	0·14792	0·19267	0·23732	0·28193	0·32652	0·37108	0·41566	0·46008	0·5031643	0·5036247	0·5040740	0·5044667	0·5052883
0·25	0·16392	0·21243	0·26051	0·30818	0·35540	0·40211	0·44825	0·49344	0·5356024	0·5359494	0·5362634	0·5364733	0·5377104
0·30	0·18254	0·23494	0·28645	0·33707	0·38671	0·43521	0·48242	0·52771	0·5678746	0·5680559	0·5681710	0·5681171	0·5700453
0·35	0·20432	0·26067	0·31554	0·36891	0·42063	0·47048	0·51818	0·56284	0·5999739	0·5999324	0·5997814	0·5993768	0·6022947
0·40	0·22986	0·29012	0·34818	0·40400	0·45739	0·50806	0·55561	0·59884	0·6319625	0·6316391	0·6311504	0·6303046	0·6344928
0·45	0·25985	0·32389	0·38485	0·44271	0·49725	0·54811	0·59478	0·63575	0·6639723	0·6633057	0·6624049	0·6610239	0·6666979
0·50	0·29504	0·36262	0·42607	0·48543	0·54048	0·59082	0·63581	0·67365	0·6962012	0·6951273	0·6937376	0·6917237	0·6989781
0·55	0·33628	0·40699	0·47239	0·53259	0·58739	0·63639	0·67886	0·71265	0·7288920	0·7273447	0·7253859	0·7226382	0·7313747
0·60	0·38443	0·45777	0·52441	0·58464	0·63833	0·68508	0·72409	0·75290	0·7622837	0·7601955	0·7575859	0·7540017	0·7638423
0·65	0·44041	0·51567	0·58271	0·64201	0·69359	0·73710	0·77167	0·79452	0·7965196	0·7938250	0·7904854	0·7859652	0·7961688
0·70	0·50505	0·58136	0·64775	0·70503	0·75339	0·79258	0·82167	0·83759	0·8315199	0·8281605	0·8240216	0·8184785	0·8279062
0·75	0·57901	0·65527	0·71980	0·77380	0·81773	0·85144	0·87398	0·88199	0·8668419	0·8627753	0·8577891	0·8511632	0·8583556
0·80	0·66256	0·73743	0·79868	0·84803	0·88623	0·91330	0·92824	0·92737	0·9016046	0·8968144	0·8909664	0·8832400	0·8866487
0·85	0·75538	0·82727	0·88365	0·92688	0·95804	0·97732	0·98367	0·97309	0·9345618	0·9290650	0·9223830	0·9135923	0·9119260
0·90	0·85635	0·92340	0·97323	1·00887	1·03175	1·04221	1·03916	1·01818	0·9643613	0·9582103	0·9507648	0·9410001	0·9335477
0·95	0·96343	1·02364	1·06522	1·09191	1·10545	1·10630	1·09326	1·06146	0·9899072	0·9831829	0·9750773	0·9644707	0·9512411
1·00	1·07374	1·12507	1·15689	1·17352	1·17698	1·16775	1·14447	1·10172	1·0106452	1·0034451	0·9947992	0·9835038	0·9651229
1·05	1·18384	1·22445	1·24531	1·25118	1·24420	1·22481	1·19142	1·13796	1·0266356	1·0190598	1·0099933	0·9981619	0·9756093
1·10	1·29016	1·31864	1·32784	1·32270	1·30537	1·27613	1·23310	1·16949	1·0384150	1·0305556	1·0211756	1·0089447	0·9832753
1·15	1·38957	1·40506	1·40244	1·38654	1·35935	1·32091	1·26899	1·19606	1·0467644	1·0386988	1·0290933	1·0165753	0·9887261
1·20	1·47967	1·48201	1·46792	1·44192	1·40567	1·35892	1·29907	1·21780	1·0524986	1·0442879	1·0345250	1·0218070	0·9925125
1·25	1·55911	1·54870	1·52393	1·48878	1·44448	1·39044	1·32368	1·23512	1·0563389	1·0480287	1·0381588	1·0253046	0·9950917
1·30	1·62747	1·60518	1·57081	1·52760	1·47633	1·41605	1·34340	1·24859	1·0588599	1·0504829	1·0405416	1·0275966	0·9968193
1·35	1·68511	1·65213	1·60935	1·55922	1·50205	1·43652	1·35892	1·25885	1·0604888	1·0520678	1·0420796	1·0290752	0·9979597

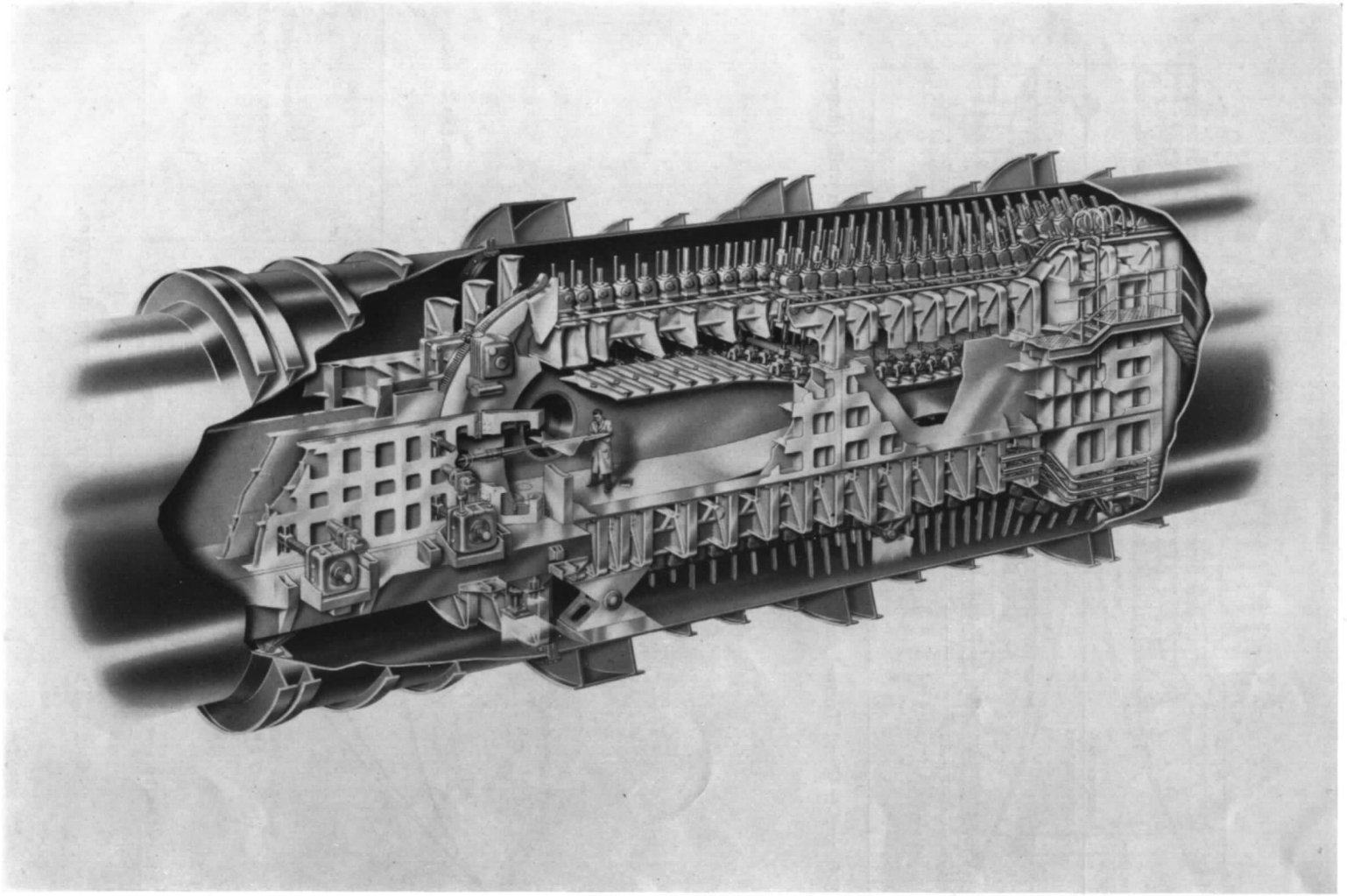

FIG. 1. R.A.E. Bedford 8-ft × 8-ft Supersonic Wind Tunnel flexible plate nozzle, model support section and supersonic diffuser.

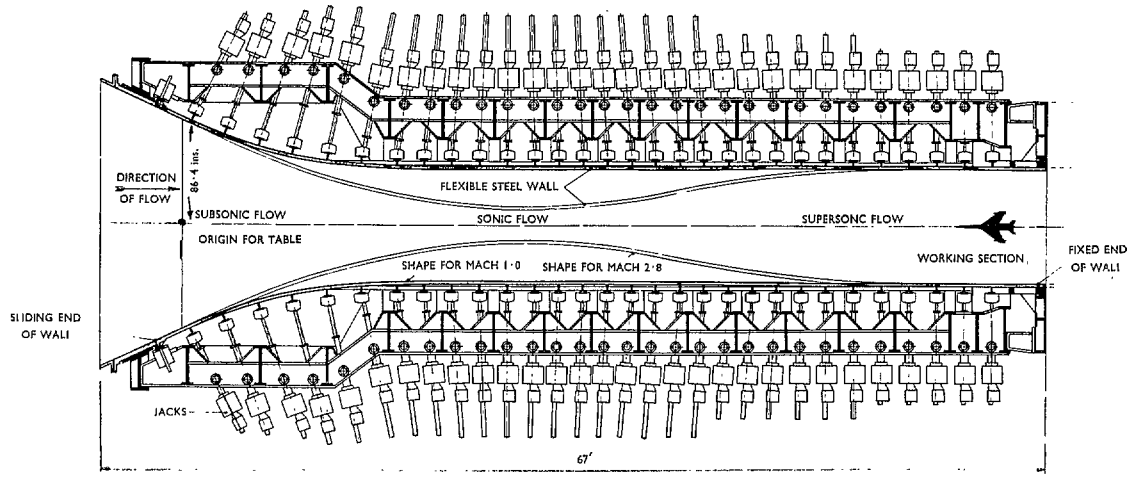

FIG. 2. The 8-ft × 8-ft Wind Tunnel at R.A.E., Bedford. Jack positions and adjustable walls (shapes for Mach 1·0 and 2·8 shown).

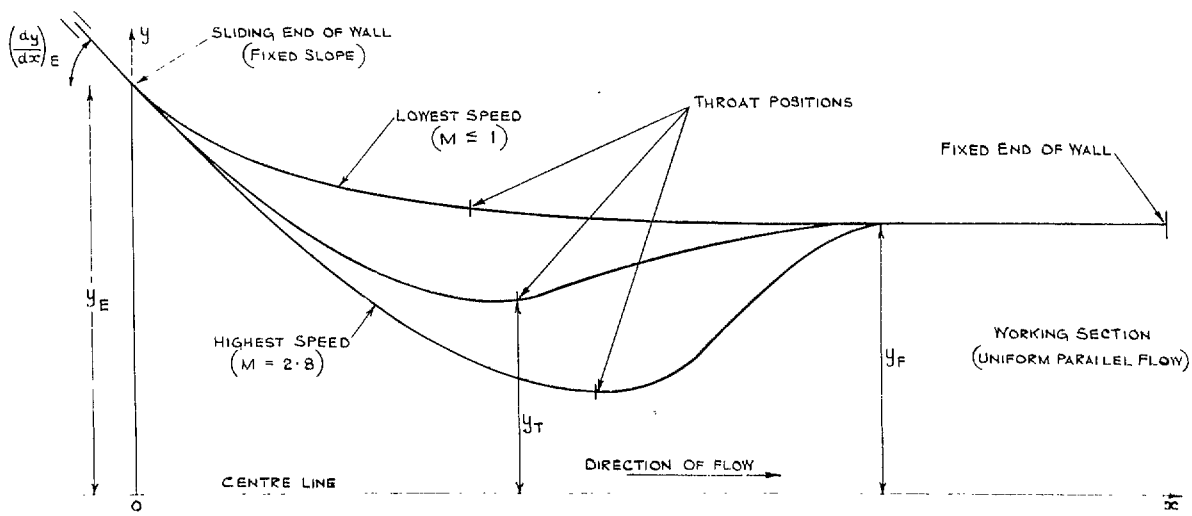

FIG. 3. The adjustable wall system: Geometry and notation.

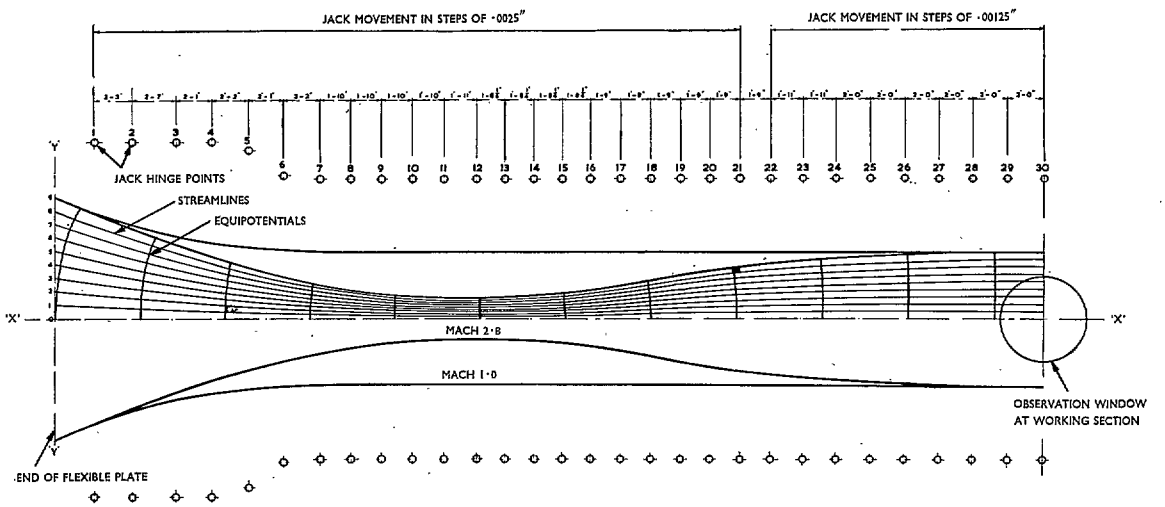

FIG. 4. The computational mesh of equipotentials and streamlines.

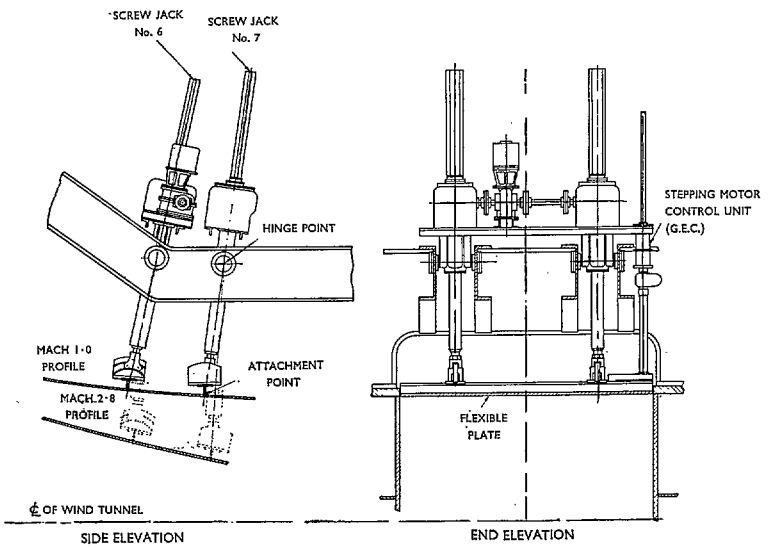

FIG. 5. Jacking system to adjust wall shape.

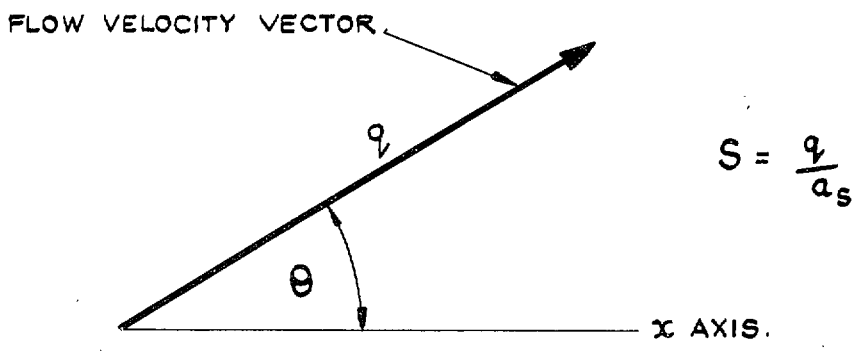

FIG. 6. The flow velocity: notation.

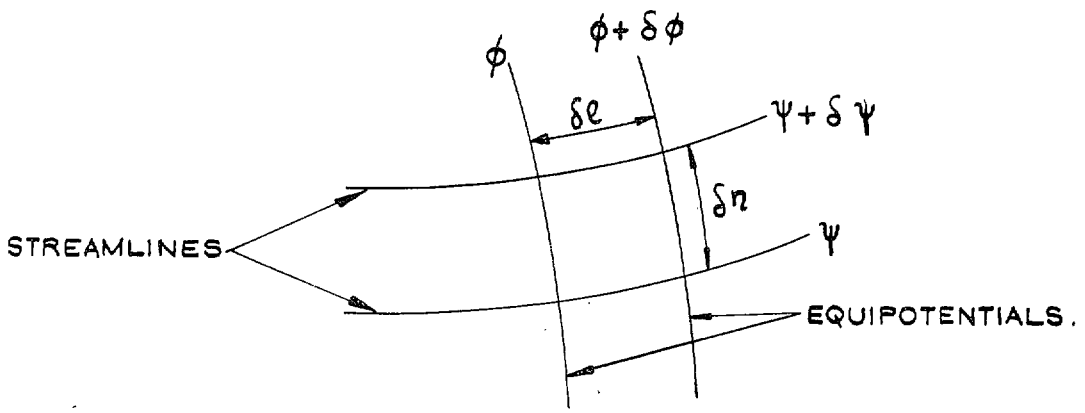

FIG. 7. Streamlines and equipotentials: notation.

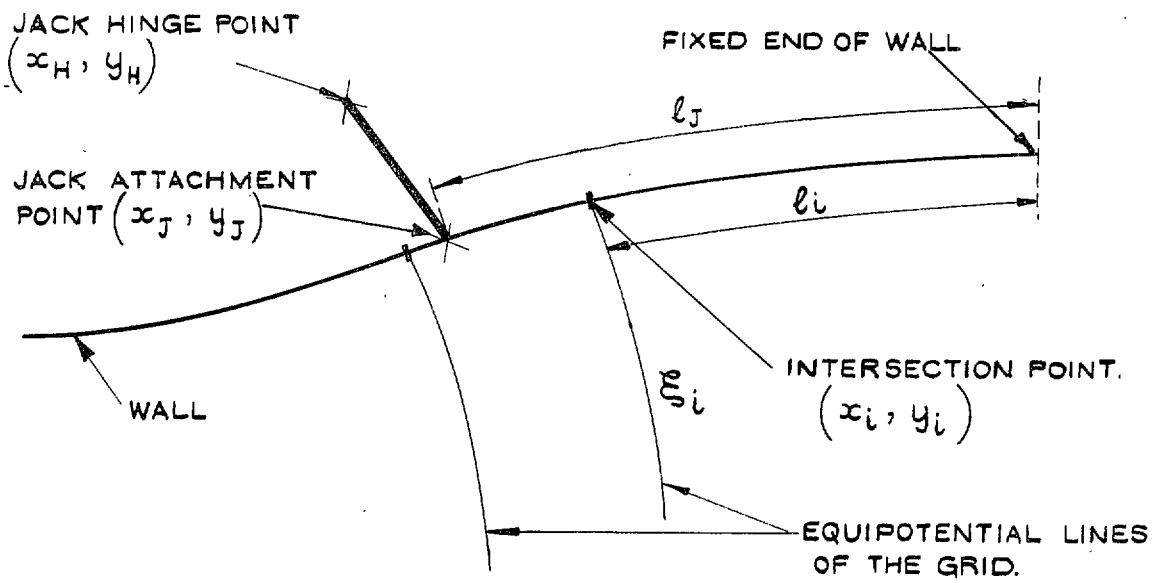

FIG. 8. Wall co-ordinates and jack extensions.

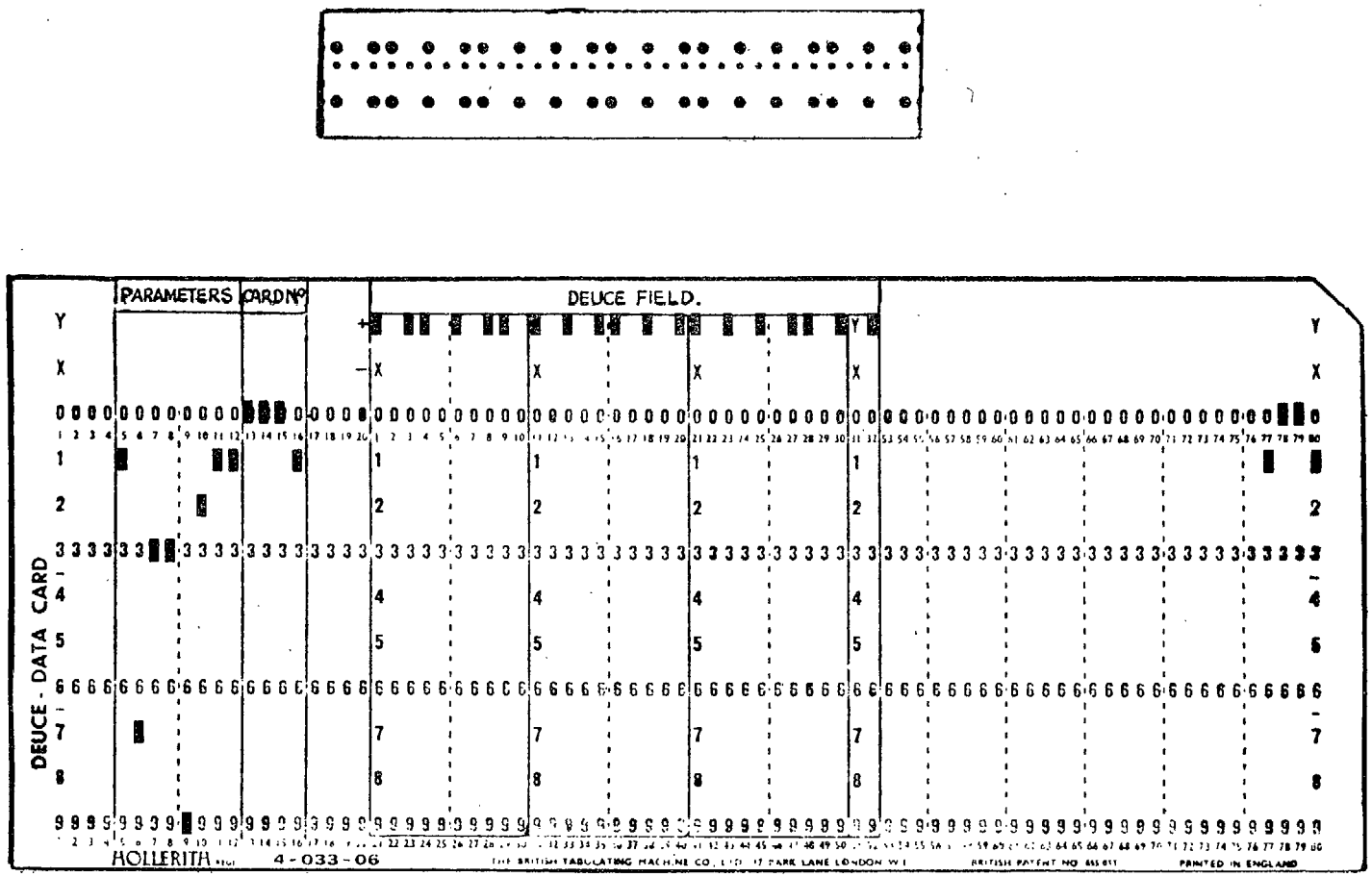

FIG. 9. Section of control tape and corresponding Hollerith Card for jack number 11.

Publications of the Aeronautical Research Council

ANNUAL TECHNICAL REPORTS OF THE AERONAUTICAL RESEARCH COUNCIL (BOUND VOLUMES)

1941 Aero and Hydrodynamics, Aerofoils, Airscrews, Engines, Flutter, Stability and Control, Structures. 63*s.* (post 2*s.* 3*d.*)

1942 Vol. I. Aero and Hydrodynamics, Aerofoils, Airscrews, Engines. 75*s.* (post 2*s.* 3*d.*)
Vol. II. Noise, Parachutes, Stability and Control, Structures, Vibration, Wind Tunnels. 47*s.* 6*d.* (post 1*s.* 9*d.*)

1943 Vol. I. Aerodynamics, Aerofoils, Airscrews. 80*s.* (post 2*s.*)
Vol. II. Engines, Flutter, Materials, Parachutes, Performance, Stability and Control, Structures. 90*s.* (post 2*s.* 3*d.*)

1944 Vol. I. Aero and Hydrodynamics, Aerofoils, Aircraft, Airscrews, Controls. 84*s.* (post 2*s.* 6*d.*)
Vol. II. Flutter and Vibration, Materials, Miscellaneous, Navigation, Parachutes, Performance, Plates and Panels, Stability, Structures, Test Equipment, Wind Tunnels. 84*s.* (post 2*s.* 6*d.*)

1945 Vol. I. Aero and Hydrodynamics, Aerofoils. 130*s.* (post 3*s.*)
Vol. II. Aircraft, Airscrews, Controls. 130*s.* (post 3*s.*)
Vol. III. Flutter and Vibration, Instruments, Miscellaneous, Parachutes, Plates and Panels, Propulsion. 130*s.* (post 2*s.* 9*d.*)
Vol. IV. Stability, Structures, Wind Tunnels, Wind Tunnel Technique. 130*s.* (post 2*s.* 9*d.*)

1946 Vol. I. Accidents, Aerodynamics, Aerofoils and Hydrofoils. 168*s.* (post 3*s.* 3*d.*)
Vol. II. Airscrews, Cabin Cooling, Chemical Hazards, Controls, Flames, Flutter, Helicopters, Instruments and Instrumentation, Interference, Jets, Miscellaneous, Parachutes. 168*s.* (post 2*s.* 9*d.*)
Vol. III. Performance, Propulsion, Seaplanes, Stability, Structures, Wind Tunnels. 168*s.* (post 3*s.* 6*d.*)

1947 Vol. I. Aerodynamics, Aerofoils, Aircraft. 168*s.* (post 3*s.* 3*d.*)
Vol. II. Airscrews and Rotors, Controls, Flutter, Materials, Miscellaneous, Parachutes, Propulsion, Seaplanes, Stability, Structures, Take-off and Landing. 168*s.* (post 3*s.* 3*d.*)

Special Volumes

Vol. I. Aero and Hydrodynamics, Aerofoils, Controls, Flutter, Kites, Parachutes, Performance, Propulsion, Stability. 126*s.* (post 2*s.* 6*d.*)
Vol. II. Aero and Hydrodynamics, Aerofoils, Airscrews, Controls, Flutter, Materials, Miscellaneous, Parachutes, Propulsion, Stability, Structures. 147*s.* (post 2*s.* 6*d.*)
Vol. III. Aero and Hydrodynamics, Aerofoils, Airscrews, Controls, Flutter, Kites, Miscellaneous, Parachutes, Propulsion, Seaplanes, Stability, Structures, Test Equipment. 189*s.* (post 3*s.* 3*d.*)

Reviews of the Aeronautical Research Council

1939–48 3*s.* (post 5*d.*) 1949–54 5*s.* (post 5*d.*)

Index to all Reports and Memoranda published in the Annual Technical Reports

1909–47 R. & M. 2600 6*s.* (post 2*d.*)

Indexes to the Reports and Memoranda of the Aeronautical Research Council

Between Nos. 2351–2449	R. & M. No. 2450 2*s.* (post 2*d.*)
Between Nos. 2451–2549	R. & M. No. 2550 2*s.* 6*d.* (post 2*d.*)
Between Nos. 2551–2649	R. & M. No. 2650 2*s.* 6*d.* (post 2*d.*)
Between Nos. 2651–2749	R. & M. No. 2750 2*s.* 6*d.* (post 2*d.*)
Between Nos. 2751–2849	R. & M. No. 2850 2*s.* 6*d.* (post 2*d.*)
Between Nos. 2851–2949	R. & M. No. 2950 3*s.* (post 2*d.*)
Between Nos. 2951–3049	R. & M. No. 3050 3*s.* 6*d.* (post 2*d.*)

HER MAJESTY'S STATIONERY OFFICE

from the addresses overleaf

Published by
HER MAJESTY'S STATIONERY OFFICE

To be purchased from
York House, Kingsway, London W.C.2
423 Oxford Street, London W.1
13A Castle Street, Edinburgh 2
109 St. Mary Street, Cardiff
39 King Street, Manchester 2
50 Fairfax Street, Bristol 1
2 Edmund Street, Birmingham 3
80 Chichester Street, Belfast 1
or through any bookseller

Printed in England

S.O. Code No. 23-3187